AUTOMATIC GUIDANCE OF FARM VEHICLES IN PRESENCE OF SLIDING EFFECTS

A SCIENTIFIC REPORT FOR THE POST-DOC RESEARCH PROJECT OF ALL-TERRAIN AUTONOMOUS VEHICLE CONTROL

Fang Hao

Nov. 2004

Abstract

High-precision autofarming is rapidly becoming a reality with the requirements of agricultural applications. Lots of research works have been focused on the automatic guidance control of farm vehicles, satisfactory results have been reported under the assumption that vehicles move without sliding. Realistic paths that farm vehicles can track successfully include not only rows but also arcs and curves. But unfortunately the pure rolling constraints are not always satisfied especially in agriculture applications where the working conditions are rough and not expectable. A possible solution would be to close the feedback loop using exteroceptive sensor measurements. Thanks to GPS and attitude sensors, vehicle positions and velocities can be obtained by absolute coordinates measurements regardless of sliding. Hence the aim of this work is to design anti-sliding controllers for all-terrain autonomous farm vehicles relying on GPS measurements.

A kinematic model which exactly integrates uncertain sliding effects is created in path frame based on geometric and velocity constraints. Through linearization, sliding appears as additive unknown variables to the ideal kinematic model, which provides a good research basis for following controller design. A three-dimensional dynamic model is constructed with Newton's laws. Sliding effects are introduced in the form of tire slip angles. Uncertainties of sliding effects are described by cornering stiffness coefficients which depend on contact conditions between tires and grounds. In order to ensure GPS-based controllers are applicable in presence of sliding, it is also proven that all the information necessary to controller design is available by either GPS measurements or reconstruction.

Thanks to the kinematic model in which sliding effects are integrated as additive disturbances, robust control theories are utilized. By transforming the vehicle-oriented kinematic model into a perturbed chained system, a sliding mode controller, which is robust not only to the sliding effects but also to the input noise, is designed with the help of the natural algebraic structure of chained systems. Simulation results show that the proposed sliding mode controller can guarantee high path-following accuracy even in the presence of sliding.

Alternatively sliding can be regarded as unknown model parameters. Based on *backstepping methods* a stepwise procedure is proposed to design an adaptive controller in which time-invariant sliding effects are learned and compensated by parameter adaptations. It is theoretically proven that for the farm vehicles subject to time-invariant sliding, the lateral deviation can be stabilized near zero and the orientation errors converge into a neighborhood near the origin. To be more robust to disturbances including external noises and unmodeled time-varying sliding components, the adaptive controller is refined by integrating Variable Structure Controllers (VSC) or projection mappings. Simulation results show that the proposed robust adaptive controllers can reject sliding effects and guarantee high lateral accuracy with about zero mean values.

For automatic guidance of agriculture vehicles, lateral control is not the only duty, the problem of longitudinal-lateral control for autonomous farm vehicles in presence of sliding is also addressed. To take sliding effects into account, two variables which characterize sliding effects are introduced into the kinematic model with respect to the vehicle body frame based on geometric and velocity constrains. With linearization approximation a refined kinematic model is obtained in which sliding appears as additive unknown parameters to the ideal kinematic model. By integrating parameter adaptation technique with *backstepping method*, a stepwise procedure is proposed to design a robust adaptive controller in which time-invariant sliding is compensated by parameter adaptation and time-varying sliding is corrected by VSC. It is theoretically proven that for the farm vehicles subjected to sliding, the longitudinal-lateral deviations can be stabilized near zero and the orientation errors converge into a neighborhood near the origin. To be more realistic for agriculture applications, an adaptive controller with projection mapping is also proposed. Simulation results show that the proposed (robust) adaptive controllers can guarantee high longitudinal-lateral tracking accuracy regardless of sliding.

Contents

Chapter 1

INTRODUCTION

1.1 Background

Precise automatic guidance and high-precision unmanned vehicle control have been the subject of research for a long time, autonomous vehicles have some benefits for production in ordinary life

- Human factors such as the driver's ability to see the ground, driver comfort and operator safety do not need to consider when designing vehicles, so the manufacture cost may be reduced.
- Remove human operators from a tired uncomfortable or dangerous working environment.
- Vehicles can run at a particular speed which guarantees the tracking accuracy without constraints of operator factors, increasing production efficiency.

Recently with the development of GPS technology, more and more researchers apply GPS to automatic guidance systems of agricultural vehicles, since GPS can provide realtime absolute position with a centimeter accuracy and outdoor working environment of agricultural vehicles is suitable for using GPS. Lots of satisfactory results of path following control have been achieved provided vehicles satisfy the pure rolling constraints [1]-[5]. In our previous works we have solved the problem of curved path following with unique RTK GPS [11], the vehicle kinematic model is created under the assumption of pure rolling, a nonlinear controller guaranteeing high lateral and orientation accuracy has been designed by converting the kinematic model into a chained system, Kalman filter is used to reconstruct system states only from GPS measurements, satisfactory results of path following have been obtained in [11] providing the vehicle moves without sliding.

However due to various effects such as slipping of tires, deformability or flexibility of wheels, the conditions of pure rolling without sliding are never strictly satisfied. Moreover with broad applications of autonomous vehicles, in lots of cases vehicles are required to be able to move on all-terrain grounds with a high accuracy. Typical terrains include stone and sand lands, grass lands and slopes where contact conditions between wheels and grounds are not ideal. When vehicles move on such grounds, inevitable occurrence of sliding violates the pure rolling constrains which are the basis of the existing controllers. Invalidation of the pure rolling assumption consequently degrades the control accuracy even system stability. But unfortunately exact models explaining internal relationship between grounds and vehicles are still unclear, so the problem of high-precision control for autonomous vehicles not satisfying pure rolling constraints provides an urgent task and challenging research subject to robotic researchers.

Until now there are very few papers dealing with sliding. [7] prevents cars from skidding by robust decoupling of car steering dynamics, but acceleration measurements are necessary and the steering angle is assumed small. [8] copes with the control of WMR (Wheeled Mobile Robot) not satisfying the ideal kinematic constraints by using slow manifold methods, but the parameter characterizing the sliding effects is assumed to be exactly known. Therefore [7][8] are not realistic for agriculture applications. In [13] a controller is designed based on the averaged model allowing the tracking errors to converge to a limit cycle near the origin. In [16] a general singular perturbation formulation is developed which leads to robust results for linearizing feedback laws ensuring trajectory tracking. But above two schemes only take into account sufficiently small skidding effects and they are too complicated for real-time practical implementation. In [14] Variable Structure Control (VSC) is used to eliminate the harmful sliding effects when the bounds of the

sliding effects have been known. The trajectory tracking problem of mobile robots in the presence of sliding is solved in [15] by using discrete-time sliding mode control. But the controllers [14]-[15] counteract sliding effects only relying on high-gain controllers which is not realistic because of limited bandwidth and low level delay introduced by steering systems of farm vehicles. In [17] sliding effects are rejected by re-scheming desired paths adaptively based on steady control errors which are mainly caused by modeled sliding effects. But [17] only care about lateral control.

1.2 Problem classification

In this report two main tasks will be completed in presence of sliding. They are classified as follows

- *Path following:* The robot must follow a geometric path in the cartesian space starting from a given initial configuration
- *Trajectory tacking:* The robot must follow a trajectory (a geometric path with an associated timing law) starting from a given initial configuration.

In path following control, time dependence is not relevant because one only concerns about the geometric displacement between the robot and the path.

In trajectory tracking tasks, robots must follow the desired path with a specified timing law (equivalently it must track a moving reference robot)

1.3 Motivation

Path following is the most general tasks in real applications, high-precision path following control can fulfill large parts of production requirements. But as refereed in last section, due to the complex principle of sliding phenomenal and inherent nonholonomic characters of autonomous vehicles, very few remarkable research results have been achieved in presence of sliding, even for path following control.

To remedy drawbacks of the previous works, in this work some controllers will be designed to ensure vehicles a high-precision guidance in presence of sliding. To meet the needs for practical applications, controllers to be proposed should have a simple structure for easy understanding, all the necessary information should be measured and reconstructed by GPS measurements. Only some reasonable assumptions are allowed to be used.

Common sense tells us that sliding effects influence vehicle motion like external disturbances, so first sliding is treated as disturbances which can be corrected by robust control. On the other hand chained system theories have advantages in controlling nonholonomic systems by transforming them into linear systems. So in this work sliding mode controllers will be applied with chained system theories to design a robust anti-sliding controller for path following.

In real world because of ground and vehicle physical characters, sliding never change too greatly with time, indeed it acts more like a time-varying model parameter alternatively. So backstepping schemes would be proposed to design an adaptive controller which can compensate time-invariant sliding. While the time-varying sliding left can be dealt with by robust controllers. In this way the undertaking of the robust controller is shared with adaptive controller which improves the path-following performance accordingly. So the robust adaptive controller is a further development of sliding mode controller we had proposed.

Based on above research works we will achieve our final target of trajectory tracking control which includes longitudinal-lateral control. Trajectory tracking control is important for drive safety control of autonomous vehicles, furthermore it is also very necessary for platoon control. In this work different from path following control, we will build the kinematic model of trajectory tacking errors in vehicle body frame, then we still rely on backstepping and robust control to achieve high-precision trajectory tracking control in presence of sliding. The results must be very meaningful for some specific applications where higher performances than path following are required.

1.4 Content and organization

In this report we investigate the problem of path following and trajectory tracking control of autonomous farm vehicles subjected to sliding. The structure of this report is that, in chapter 2 a general kinematic and dynamic model are constructed in presence of sliding, the problem of parameter reconstruction with GPS is investigated also. In chapter 3 by transforming the vehicle-oriented kinematic model into a chained form, a new sliding mode controller is designed and the stability of the closed-loop system is proven. In chapter 4 an adaptive controller is designed first for lateral control by using backstepping schemes, then either variable structure control or projection mapping is applied to refine the adaptive controller to make it robust to the unmodelled sliding. In chapter 5 the robust adaptive controller proposed in chapter 4 is extended to design a longitudinal-lateral controller, it is theoretically proven that the longitudinal-lateral deviations are stabilized around zero, the orientation errors converge into a neighborhood near the origin. Furthermore the controller is simplified into an ordinary adaptive controller with projection mapping for the purpose of providing a realistic motion.

Chapter 2

KINEMATIC AND DYNAMIC MODELING OF VEHICLES SUBJECTED TO SLIDING EFFECTS

In this chapter we investigate kinematic and dynamic modeling of vehicles that are subjected to sliding effects. In section 2.1 based on geometric relationships and velocity constraints a kinematic model is built in the path frame which integrates sliding effects exactly, then linear approximation is used to make sliding appear as additive variables to the ideal kinematic model. In section 2.2 using Newton's law, a 3-dof dynamic model is constructed which enable one to describe full vehicle motions in $x-y$ plane. To be convenient for designing anti-sliding controllers, a linear tire model is used to describe sliding effects. Uncertainties of sliding effects are described by a single unknown cornering stiffness coefficient. In section 2.3 a two-antenna GPS receiver is proposed to obtain the knowledge of all the state variables. It is also proven that incline angles of slopes, the important parameter for mobility analysis, can be reconstructed by a single GPS.

2.1 Kinematic model

2.1.1 Notation and Problem Description

In this chapter the vehicle is simplified into a bicycle model. The kinematic model is expressed with respect to the path in frame (M, η_t, η_n), variables necessary in the kinematic model are denoted as follows: (see figure 2.1)

- C is the path to be followed.
- O is the center of the vehicle virtual rear wheel.
- M is the orthogonal projection of O on path C.
- η_t is the tangent vector to the path at M.
- η_n is the normal vector at M.
- y is the lateral deviation between O and M
- s is the curvilinear coordinates (arc-length) of point M along the path from an initial position.
- $c(s)$ is the curvature of the path at point M.
- $\theta_d(s)$ is the orientation of the tangent to the path at point M with respect to the inertia frame.
- θ is the orientation of the vehicle centerline with respect to the inertia frame.

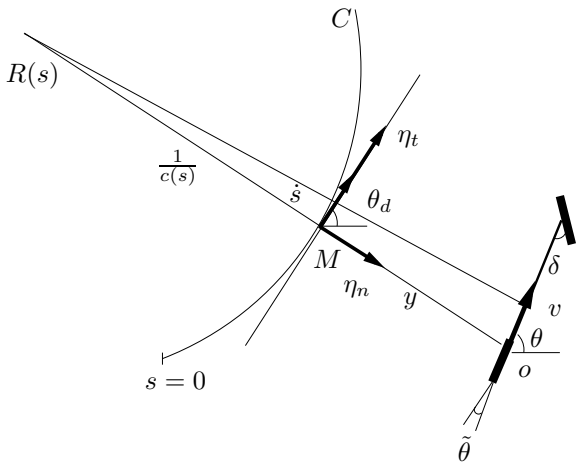

Figure 2.1: Notation and path frame description

- $\tilde{\theta} = \theta - \theta_d$ is the orientation error.
- l is the vehicle wheelbase.
- v is the vehicle linear longitudinal velocity.
- δ is the steering angle of the virtual front wheel

So the vehicle movement can be described by $(y, s, \tilde{\theta})$ with respect to the path frame.

2.1.2 Kinematic Model

When the vehicles move without sliding, the ideal kinematic model of the vehicles is (see [11]).

$$\begin{cases} \dot{s} = \dfrac{v\cos\tilde{\theta}}{1 - c(s)y} \\ \dot{y} = v\sin\tilde{\theta} \\ \dot{\tilde{\theta}} = v\Big(\dfrac{\tan\delta}{l} - \dfrac{c(s)\cos\tilde{\theta}}{1 - c(s)y}\Big) \end{cases} \tag{2.1}$$

But when the vehicles move on a steep slope or the ground is slippery, sliding occurs inevitably, (2.1) is no longer valid. The violation of the pure rolling constraints is described by introducing the lateral slip velocity v_y and steering angle bias δ_b (figure 2.2). From figure 2.2 the desired angular velocity is obtained

$$\dot{\theta}_d = v\frac{\tan(\delta + \delta_b)}{l} - \frac{v_y}{l} \tag{2.2}$$

Similar developing methods lead to

$$\dot{\theta}_c = \frac{\dot{s}}{\frac{1}{c(s)}} = \frac{v\cos\tilde{\theta} - v_y\sin\tilde{\theta}}{\frac{1}{c(s)} - y} \tag{2.3}$$

It is also obtained that

$$\dot{y} = v\sin\tilde{\theta} + v_y\cos\tilde{\theta} \tag{2.4}$$

Collecting (2.2)(2.3)(2.4) provides a kinematic model integrating sliding precisely

$$\begin{cases} \dot{s} = \dfrac{v\cos\tilde{\theta}}{1 - c(s)y} - \dfrac{v_y\sin\tilde{\theta}}{1 - c(s)y} \\ \dot{y} = v\sin\tilde{\theta} + v_y\cos\tilde{\theta} \\ \dot{\tilde{\theta}} = v\Big(\dfrac{\tan(\delta + \delta_b)}{l} - \dfrac{c(s)\cos\tilde{\theta}}{1 - c(s)y}\Big) - \dfrac{v_y}{l} + \dfrac{c(s)v_y\sin\tilde{\theta}}{1 - c(s)y} \end{cases} \tag{2.5}$$

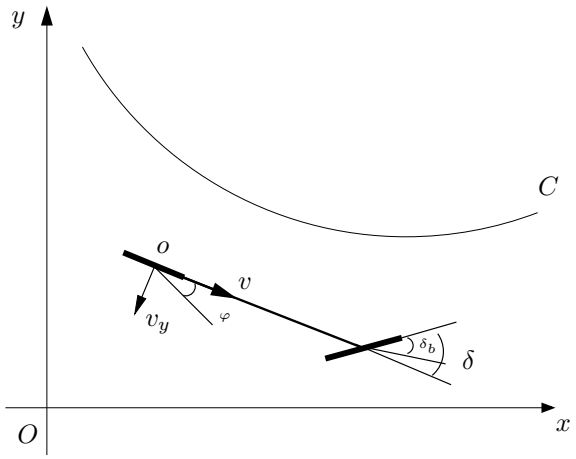

Figure 2.2: Notations of sliding effects

In above kinematic model the steering bias δ_b is included together with δ in function $\tan(\cdot)$. But since δ_b is quite small, a linearized kinematic model can be obtained

$$\begin{cases} \dot{s} = \dfrac{v\cos\tilde{\theta}}{1-c(s)y} - \dfrac{\psi(t)\sin\tilde{\theta}}{1-c(s)y} \\ \dot{y} = v\sin\tilde{\theta} + \psi(t)\cos\tilde{\theta} \\ \dot{\tilde{\theta}} = v\Big(\dfrac{\tan\delta}{l} - \dfrac{c(s)\cos\tilde{\theta}}{1-c(s)y}\Big) + \dfrac{v}{l}\eta(t) + \big(\dfrac{c(s)\sin\tilde{\theta}}{1-c(s)y} - \dfrac{1}{l}\big)\psi(t) \end{cases} \tag{2.6}$$

where $\psi(t) = v_y$, $\eta(t)$ is linked to δ_b including inaccuracy due to linearization approximation. In above kinematic model it is noticed that all the sliding effects appear as the additive unknown variables to the ideal kinematic model. This linearized kinematic model provides a right basis for the following procedure of controller design.

2.2 Dynamic model

2.2.1 Notations and assumption

Kinematic-based model is a simple method to cope with sliding, but dynamic analysis is rather necessary when heavy vehicles move on a slope and follow a curved path with enough high speeds.

We have known that the most simplified vehicle dynamic model is the two-degree-freedom bicycle model. This model represents the lateral and yaw motions but not considering the longitudinal direction, because it does not affect the lateral and yaw stability. Most approaches developed to remedy sliding effects assume the longitudinal velocity to be constant [26][27]. But in real cases it is not always true especially when vehicles move on slopes. In order to perform longitudinal control as well, a three-degree-freedom model is built in this section adding longitudinal acceleration into the model, therefore enabling one to describe the full vehicle motions in $X-Y$ plane.

In order to build the dynamic model, it is necessary to analyze the forces that actuate on the vehicle. The external forces acting on the vehicle consist of the friction forces between the vehicle and ground, the normal forces, the gravity and the control force. All the forces vertical to the slope are not considered, so the external forces acting in the slope $O-X'Y'$ is shown in figure (2.3). In this figure $O-XYZ$ is the inertia coordinates, $O-X'Y'Z'$ is the fixed slope coordinates. They are constructed such that OZ, OZ', OX' lay in a common vertical plane. OZ' is normal to the slope. $o-xyz$ is the body coordinates consisting with the heading of the vehicle, β is the incline angle of the slope, $mg\sin\beta$ is the component of the gravity parallel to OX', the lateral tire force f_f, f_r, acting on the front and rear wheels are defined by a linear tire model.

$$\begin{cases} f_f(\delta_b) = c_f\delta_b \\ f_r(\varphi) = c_r\varphi \end{cases} \tag{2.7}$$

where δ_b, φ are the slip angles of the front and rear wheels defined by figure 2.2. $c_f = \mu c_{f0}$ and $c_r = \mu c_{r0}$ are the cornering stiffness coefficients of the tires that vary with road tire contact, c_{f0} and c_{r0} are the nominal values of the cornering stiffness for the dry roads, $\mu \in [u^-,\ 1]$ is an uncertain variable depending on the road condition, for example on dry concrete roads $\mu = 1$; while on wet grass roads $\mu = \mu^-$. F is the longitudinal control force whose maximum value is determined by engine output capabilities and road conditions. It can be used for several purposes: overcoming road loads, maneuvering (trajectory following) and correcting parameter errors.

In our applications GPS is used to guide vehicles with centimeter accuracy in the absolute coordinates frame. The GPS antenna is mounted on the top of the vehicle straight up the center of the rear axle, so we use the middle point of the rear axle p as the reference point to build the dynamic model.

As all the external forces acting in the slope can be projected onto longitudinal and lateral forces f_x and f_y with respect to the body coordinates, in $o - xyz$ one has

$$\begin{pmatrix} f_x \\ f_y \\ m_z \end{pmatrix} = \begin{pmatrix} -\sin\delta & 0 \\ \cos\delta & 1 \\ l_f\cos\delta & -l_r \end{pmatrix} \begin{pmatrix} f_f \\ f_r \end{pmatrix} + \begin{pmatrix} F \\ 0 \\ 0 \end{pmatrix} + \begin{pmatrix} -mg\sin\beta\cos\theta \\ mg\sin\beta\sin\theta \\ 0 \end{pmatrix} \tag{2.8}$$

where δ is the steering angle of the front wheel, θ is the orientation angle between axis OX' and ox.

The velocity and geometry notations of the vehicle are shown in figure (2.4). In this figure v_r is the translational velocity of the reference point p, $v_x = v_r\cos\varphi$ and $v_y = v_r\sin\varphi$ are the longitudinal and lateral velocity components. Because the GPS antenna is mounted straight up p, v_r can be measured directly from the GPS signals. The wheel slip angles δ_b φ can be determined by

$$\begin{aligned} \delta_b &= \delta - \frac{l\omega + v_y}{v_x} \\ \varphi &= \frac{v_y}{v_x} \end{aligned} \tag{2.9}$$

where $\omega = \dot{\theta}$ is the raw rate around the mass center. $l = l_r + l_f$ is the wheel span.

2.2.2 Dynamic model

Applying Newton's law for the mass center in $o - xyz$ coordinates frame, we have on the ox

$$m\ddot{x} - m\dot{y}\omega = f_x \tag{2.10}$$

and on the oy

$$m\ddot{y} + m\dot{x}\omega = f_y \tag{2.11}$$

The yaw motion around the mass center is described by

$$I_z\dot{\omega} = M_z \tag{2.12}$$

where $I_z = ml_fl_r$. From the velocity constraints between the mass center and point p, we have

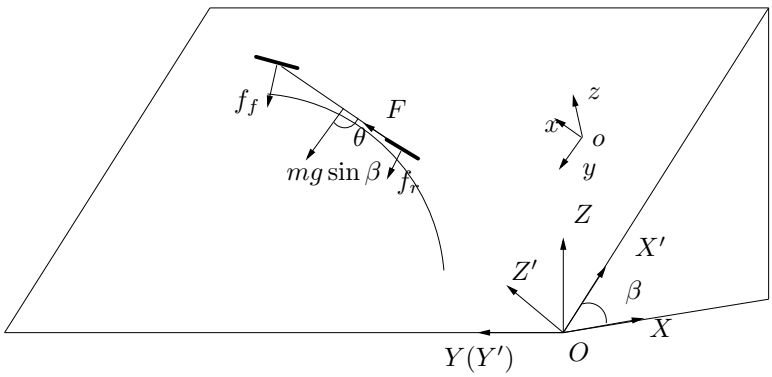

Figure 2.3: External force

$$\begin{aligned}\dot{x} &= v_x \\ \ddot{x} &= \dot{v}_x \\ \dot{y} &= v_y + l_r\omega \\ \ddot{y} &= \dot{v}_y + l_r\dot{\omega}\end{aligned} \tag{2.13}$$

Substituting (2.13) into (2.10)(2.11), the dynamic model for point p is obtained

$$\begin{aligned}m\dot{v}_x - m(v_y + l_r\omega)\omega &= f_x \\ m(\dot{v}_y + l_r\dot{\omega}) + mv_x\omega &= f_y\end{aligned} \tag{2.14}$$

Generally the desired path which the vehicle is going to follow is defined in the slope coordinates frame, for example by a curvature of a circle or a straight line in $O - X'Y'$, so it is feasible to define the attitude variables of the dynamic model in the slope coordinates frame $O - X'Y'$, while the velocity variables are defined in the body coordinates frame $o - xy$.

- $x_1 = X'_p$ the coordinates of p in OX'
- $x_2 = Y'_p$ the coordinates of p in OY'
- $x_3 = \theta$ the orientation angle with respect to $O - X'Y'$
- $x_4 = v_x$ the longitudinal velocity of p with respect to $o - xy$
- $x_5 = v_y$ the lateral velocity of p with respect to $o - xy$
- $x_6 = \omega$ the yaw rate of the vehicle around the mass center

The lateral and longitudinal velocities of point p with respect to the slope coordinates $O - X'Y'Z'$ can be described as follow:

$$\begin{aligned}\dot{X}'_p &= v_x\cos\theta - v_y\sin\theta \\ \dot{Y}'_p &= v_x\sin\theta + v_y\cos\theta\end{aligned} \tag{2.15}$$

So the three-degree-of-freedom vehicle dynamic models (2.12)(2.14) are rewritten in form of first order differential equations, to enable using the first-order numerical integration method, such as Runge-Kutta. The state space representation of the dynamic model is

$$\begin{aligned}\dot{x}_1 &= x_4\cos x_3 - x_5\sin x_3 \\ \dot{x}_2 &= x_4\sin x_3 + x_5\cos x_3 \\ \dot{x}_3 &= x_6 \\ \dot{x}_4 &= l_r x_6^2 + x_5x_6 + \frac{-\sin\delta f_f + F - mg\sin\beta\cos x_3}{m} \\ \dot{x}_5 &= -l_r\dot{x}_6 - x_4x_6 + \frac{\cos\delta f_f + f_r + mg\sin\beta\sin x_3}{m} \\ \dot{x}_6 &= \frac{l_f\cos\delta f_f - l_r f_r}{I_z}\end{aligned} \tag{2.16}$$

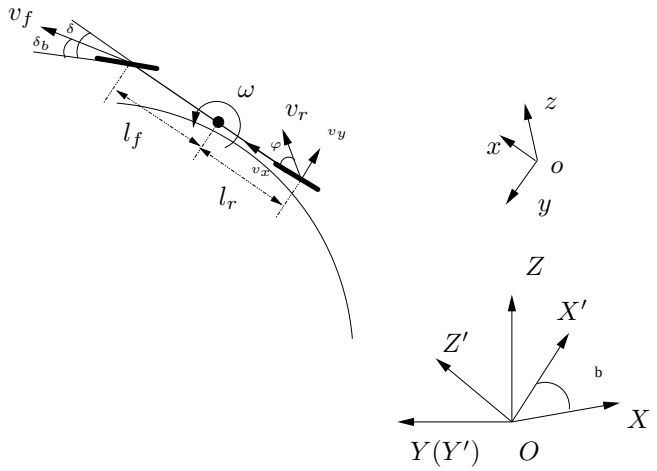

Figure 2.4: Velocity and geometry notations

In this dynamic model the control inputs are the longitudinal control force F and the steering angle δ. From (2.7)(2.9), one has that

$$\dot{x}_4 = \frac{F - mg\sin\beta\cos x_3}{m} + x_5 x_6 - \frac{\sin\delta(\delta - \frac{lx_6 + x_5}{x_4})}{m} c_f + l_r x_6^2 \tag{2.17}$$

$$\dot{x}_5 = \frac{mg\sin\beta\sin x_3}{m} - x_4 x_6 + \frac{x_5}{x_4 m} c_r + \frac{\cos\delta(\delta - \frac{lx_6 + x_5}{x_4})}{m} c_f - l_r \dot{x}_6 \tag{2.18}$$

$$\dot{x}_6 = \frac{l_f \cos\delta(\delta - \frac{lx_6 + x_5}{x_4})}{I_z} c_f - \frac{l_r c_r x_5}{I_z x_4} \tag{2.19}$$

If the steering angle δ is so small that $\sin\delta \approx 0$, $\cos\delta \approx 1$, then the dynamic model is

$$\dot{x}_1 = x_4\cos x_3 - x_5\sin x_3 \tag{2.20}$$

$$\dot{x}_2 = x_4\sin x_3 + x_5\cos x_3 \tag{2.21}$$

$$\dot{x}_3 = x_6 \tag{2.22}$$

$$\dot{x}_4 = -g\sin\beta\cos x_3 + x_5 x_6 + \frac{F}{m} + l_r x_6^2 \tag{2.23}$$

$$\dot{x}_5 = g\sin\beta\sin x_3 - x_4 x_6 + \frac{\mu c_{f0}}{m}\delta - \frac{\mu c_{f0} l x_6}{m x_4} + \mu(\frac{c_{r0}}{m} - \frac{c_{f0}}{m})\frac{x_5}{x_4} - l_r \dot{x}_6 \tag{2.24}$$

$$\dot{x}_6 = \mu\big(\frac{l_f c_{f0}}{I_z}\delta - \frac{l_f c_{f0} l x_6}{I_z x_4} - \frac{(l_r c_{r0} + l_f c_{fo})x_5}{I_z x_4}\big) \tag{2.25}$$

This dynamic model is nonlinear, coupled and nonholonomic. All the state variables can be measured or reconstructed (see section 2.3) except for μ which describes uncertainties of sliding effects. It cannot be measured exactly or known previously, so in our model it is treated as the uncertain parameter. To track the desired path as closely as possible, plenty of research results in robust control and adaptive control can be relied on to cope with the uncertainty of μ [20].

2.3 State variable estimation and coordinates transformation

Incline angles of slopes have profound effects on vehicle performance; even modest incline angles may be a quite challenge for vehicles with low power-to-weight ratio. Thus knowledge of incline angles is essential to ensure vehicle mobility. In this chapter the incline angle is obtained relying on a single GPS. When vehicles move on a slope, the GPS coordinates are sampled at three different points p_i $(i = 1, 2, 3)$. The normal vector n to the slope is obtained by

$$n = p_1 p_2 \times p_1 p_3 \tag{2.26}$$

Since the angle between vector n and $[0, 0, 1]$ is equal to the incline angle β, so we have

$$\beta = \cos^{-1}(\frac{n}{|n|} \cdot [0, 0, 1]) \tag{2.27}$$

When vehicles are subjected to sliding effects, the direction of the translational velocity will deviate from the heading of the body axis because of the wheel slip, so the orientation of the vehicle body cannot be reconstructed anymore with the velocity information derived from a single GPS [32]. There are two solutions to this problem. The first one is using a yaw gyro to measure the vehicle body heading (yaw). The gyro can provide higher update rates for estimating yaw angle than GPS, but the gyro biases which cannot be known exactly may result in significant estimation errors. Another solution is utilizing a two-antenna GPS receiver. In this application two antennas are located on top of the vehicle longitudinally, so the body pitch angle λ with respect to the horizontal plane can be obtained easily by

$$\lambda = \tan^{-1}\frac{|Z_2 - Z_1|}{\sqrt{(X_2 - X_1)^2 + (Y_2 - Y_1)^2}} \tag{2.28}$$

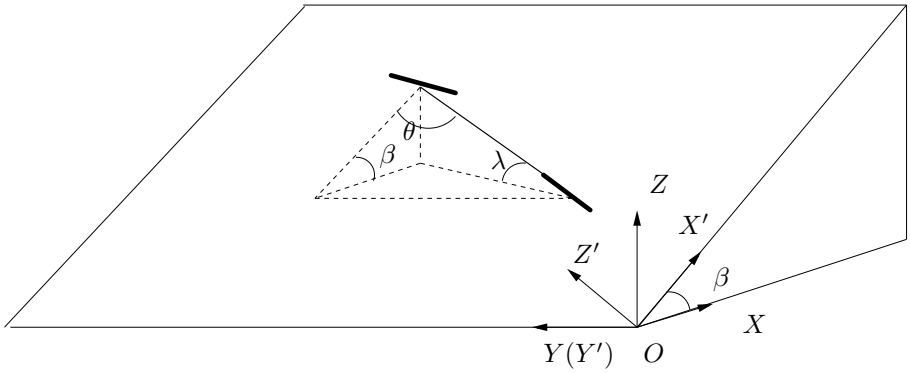

Figure 2.5: Geometric relationship

(X_i, Y_i, Z_i) are the coordinates of ith GPS antenna. From the geometric relationships shown in figure (2.5), the yaw angle of the vehicles with respect to the frame $O - X'Y'Z'$ can be calculated as follow

$$\theta = \cos^{-1}(\frac{\sin\lambda}{\sin\beta}) \tag{2.29}$$

The coordinates frames used in this application are shown is figure (2.6). Generally in practice the desired states that the vehicle is going to follow are defined in the slope coordinates $O - X'Y'Z'$ for convenience, while the information from GPS is in the absolute frame which can be transferred into $O - XYZ$ easily, so it is very necessary to transfer the coordinates from $O - XYZ$ into $O - X'Y'Z'$.

The coordinates of the reference point in frame $O - X'Y'Z'$ are deduced by

$$\begin{pmatrix} X' \\ Y' \\ Z' \end{pmatrix} = \begin{pmatrix} \cos\beta & 0 & \sin\beta \\ 0 & 1 & 0 \\ -\sin\beta & 0 & \cos\beta \end{pmatrix} \begin{pmatrix} X \\ Y \\ Z \end{pmatrix} \tag{2.30}$$

If assume the incline angle β is constant, the velocity vector in $O - X'Y'Z'$ is

$$\begin{pmatrix} \dot{X}' \\ \dot{Y}' \\ \dot{Z}' \end{pmatrix} = \begin{pmatrix} \cos\beta & 0 & \sin\beta \\ 0 & 1 & 0 \\ -\sin\beta & 0 & \cos\beta \end{pmatrix} \begin{pmatrix} \dot{X} \\ \dot{Y} \\ \dot{Z} \end{pmatrix} \tag{2.31}$$

After coordinates transformation from $O - X'Y'Z'$ into $o - xyz$, the coordinates of the reference point in the rotating body coordinates frame is

$$\begin{pmatrix} x \\ y \\ z \end{pmatrix} = \begin{pmatrix} \cos\theta & \sin\theta & 0 \\ -\sin\theta & \cos\theta & 0 \\ 0 & 0 & 1 \end{pmatrix} \begin{pmatrix} X' \\ Y' \\ Z' \end{pmatrix} \tag{2.32}$$

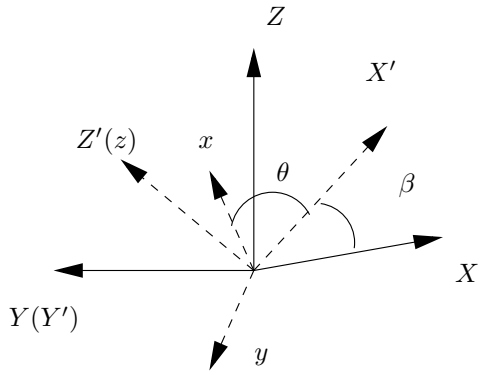

Figure 2.6: Coordinates frames

From (2.30) and (2.32) we get

$$\begin{pmatrix} x \\ y \\ z \end{pmatrix} = A \begin{pmatrix} X \\ Y \\ Z \end{pmatrix} \tag{2.33}$$

where

$$A = \begin{pmatrix} \cos\theta\cos\beta & \sin\theta & \cos\theta\sin\beta \\ -\sin\theta\cos\beta & \cos\theta & -\sin\theta\sin\beta \\ -\sin\beta & 0 & \cos\beta \end{pmatrix} \tag{2.34}$$

So for the reference point p the velocity vector in the body coordinates frame is

$$\begin{pmatrix} v_x \\ v_y \\ v_z \end{pmatrix} = \begin{pmatrix} \dot{x}_p \\ \dot{y}_p \\ \dot{z}_p \end{pmatrix} = A \begin{pmatrix} \dot{X}_p \\ \dot{Y}_p \\ \dot{Z}_p \end{pmatrix} + B \begin{pmatrix} X_p \\ Y_p \\ Z_p \end{pmatrix} \tag{2.35}$$

where

$$B = \begin{pmatrix} -\sin\theta\cos\beta\omega & \cos\theta\omega & -\sin\theta\sin\beta\omega \\ -\cos\theta\cos\beta\omega & -\sin\theta\omega & -\cos\theta\sin\beta\omega \\ 0 & 0 & 0 \end{pmatrix} \tag{2.36}$$

Thus all the state variables used in the dynamic model $X', Y', \theta, v_x, v_y, \omega$ and the incline angle of the slope β, which is the most important parameter for vehicle mobility, can be obtained by direct measurement and reconstruction using a two-antenna GPS receiver.

2.4 Conclusion

Sliding inevitably occurs when vehicles move in a slippery environment which degrades the path following accuracy significantly. To correct the sliding effects, using geometry relationship and velocity constraints a kinematic model is built in which sliding effects are described by lateral sliding velocity and steering bias. The resulting model integrates the sliding effects exactly from kinematic constraints point of view. Furthermore the kinematic model is linearized which make it quite straightforward to design anti-sliding controllers.

Based on Newton's law, the dynamic model is constructed. Different from pure rolling conditions, the sliding effects are introduced into the models by tire forces which have linear relationships with wheel slip angles. Uncertainties of sliding effects are formulated by an unknown cornering stiffness coefficient. By regarding it as uncertainties in dynamic models, lots of nonlinear control methods such as robust control and adaptive control can be relied on to remedy it. When sliding effects are taken into account, some vehicle states for example the orientation angle cannot be obtained by only one GPS receiver, so a two-antenna GPS system is proposed. With this new GPS system, all the state variables in the models can be measured or reconstructed. It is also proven that incline angles of slopes which play a very important role in dynamic mobility can be estimated by a single GPS.

Chapter 3

PATH FOLLOWING CONTROL BASED ON SLIDING MODE CONTROLLER

It has been well known that vehicle positions and velocities cannot be measured by relative localization systems for example incremental encoders when sliding occurs, so absolute localization is necessary for anti-sliding control. The absolute localization technologies include active beacon, GPS, laser range scans and multi-sensor data fusion etc. In addition, with the development of GPS technology more and more researchers apply GPS to automatic guidance systems of agricultural vehicles [9]-[12], since GPS can provide realtime *absolute* positions with centimeter accuracy and outdoor working environments of agricultural vehicles are suitable for using GPS. Due to those two points and our previous works [11], in the following chapters the problem of anti-sliding controller design will be addressed for the farm vehicles with GPS localization systems.

The main idea of this chapter is regarding sliding effects as additive disturbances to the ideal kinematic model, then theories of sliding mode control are used to design a robust controller which has ability to reject sliding effects from the vehicle's path following performance. The structure of this chapter is that, in section 3.1 a vehicle-oriented kinematic model considering sliding is built in the path frame. In section 3.2 chained system properties are reviewed by recalling our previous works. In section 3.3 by transforming the vehicle-oriented kinematic model into a chained form, a new sliding mode controller is designed and the stability of the closed-loop system is proven. In section 3.4, some comparative simulation results are presented to validate the proposed control law.

3.1 Kinematic model

3.1.1 Notation and problem description

For simplicity the vehicle is simplified with a bicycle model such that the two actual front wheels are equivalent to a unique virtual wheel located at the mid-distance between the actual wheels. The angle between the axis of the front wheels and the vehicle body is called the steering angle δ which is adjusted to allow the vehicle to follow the desired path. The direction of the rear wheels is fixed along the body axis.

In this chapter the kinematic model is expressed with respect to the path in frame (M, η_T, η_N), variables necessary in the kinematic model are denoted as follow: (see figure 3.1)

- C is the path to be followed.
- O is the center of the vehicle virtual rear wheel.
- M is the orthogonal projection of O on path C, M exits and is uniquely defined if the path meets some conditions.
- η_T is the tangent vector to the path at M.

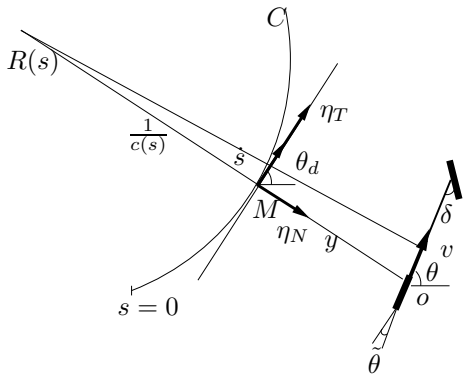

Figure 3.1: Notation and path frame description

- η_N is the normal vector at M.
- y is the lateral deviation between O and M
- s is the curvilinear coordinates (arc-length) of point M along the path from an initial position.
- $c(s)$ is the curvature of the path at point M.
- θ_d is the orientation of the tangent to the path at point M.
- θ is the orientation of the vehicle centerline with respect to the inertia frame.
- $\tilde{\theta} = \theta - \theta_d$ is the orientation error.
- l is the vehicle wheelbase.
- v is the vehicle linear longitudinal velocity.
- δ is the steering angle of the virtual front wheel

So the new set of state vectors in the path frame is $(y, s, \tilde{\theta})$, the path following problem consists of finding a feedback control law

$$\delta = K(s, y, \tilde{\theta}, v) \tag{3.1}$$

such that

$$\lim_{t\to\infty} y = 0 \tag{3.2}$$

and $\tilde{\theta}$ is bounded in presence of sliding

3.1.2 Kinematic model

In section 2.1.2 we have obtained a linearized kinematic model with sliding in the path frames as follows

$$\begin{cases} \dot{s} = \dfrac{v\cos\tilde{\theta}}{1-c(s)y} - \dfrac{\psi(t)\sin\tilde{\theta}}{1-c(s)y} \\ \dot{y} = v\sin\tilde{\theta} + \psi(t)\cos\tilde{\theta} \\ \dot{\tilde{\theta}} = v\Big(\dfrac{\tan\delta}{l} - \dfrac{c(s)\cos\tilde{\theta}}{1-c(s)y}\Big) + \dfrac{v}{l}\eta(t) + \big(\dfrac{c(s)\sin\tilde{\theta}}{1-c(s)y} - \dfrac{1}{l}\big)\psi(t) \end{cases} \tag{3.3}$$

where $\psi(t)$ equals to the lateral sliding velocity v_y, $\eta(t)$ is linked to the steering bias δ_b. In this model it is noticed that all the sliding effects take effects like unknown additive variables. To take advantage of such a structure, we treat sliding effects $\psi(t)$ and $\eta(t)$ as external disturbances, then we have

$$\begin{cases} \dot{s} = \dfrac{v\cos\tilde{\theta}}{1-c(s)y} + \varepsilon_1 \\ \dot{y} = v\sin\tilde{\theta} + \varepsilon_2 \\ \dot{\tilde{\theta}} = v\Big(\dfrac{\tan\delta}{l} - \dfrac{c(s)\cos\tilde{\theta}}{1-c(s)y}\Big) + \varepsilon_3 \end{cases} \tag{3.4}$$

where ε is the vector depicting the violation of the ideal rolling without sliding constraints, ε is bounded by a known constant γ, that is $|\varepsilon_i| \leq \gamma_i$.

In actual applications, the longitudinal friction is much larger than the sliding force and the longitudinal velocity varies slowly enough, so in this chapter the sliding effect ε_1 in the longitudinal direction is negligible, the vehicle-oriented kinematic model is rewritten as

$$\begin{cases} \dot{s} = \dfrac{v\cos\tilde{\theta}}{1-c(s)y} \\ \dot{y} = v\sin\tilde{\theta} + \varepsilon_2 \\ \dot{\tilde{\theta}} = v\Big(\dfrac{\tan\delta}{l} - \dfrac{c(s)\cos\tilde{\theta}}{1-c(s)y}\Big) + \varepsilon_3 \end{cases} \tag{3.5}$$

3.2 Previous works

3.2.1 Chained system properties

As presented in [11], in our previous work a path following controller has been designed by converting the model (2.1) into a chained system which allows using linear system theories to design nonlinear controllers without any approximation while still relying on the actual nonlinear system model (see [2]). For a 3-D nonlinear system with two control inputs, the general chained system is written as

$$\text{derivation w.r.t } \boldsymbol{t} \begin{cases} \dot{a}_1 = m_1 \\ \dot{a}_2 = a_3 m_1 \\ \dot{a}_3 = m_2 \end{cases} \tag{3.6}$$

where $A = [a_1, a_2, a_3]$ and $M = [m_1, m_2]$ are respectively the states and control inputs of the chained system. The general chained system can be converted into a single-input linear system by replacing the time derivative with a derivation with respect to the state variable a_1. Using the notation

$$\frac{d}{da_1}a_i = a_i' \quad and \quad m_3 = \frac{m_2}{m_1} \tag{3.7}$$

the general chained system is changed into

$$\text{derivation w.r.t } \boldsymbol{a}_1 \begin{cases} a_1' = 1 \\ a_2' = a_3 \\ a_3' = m_3 \end{cases} \tag{3.8}$$

where m_3 is the virtual control input.

3.2.2 Automatic guidance based on chained form system

Considering the kinematic model (2.1), via state transformation as following

$$(a_1, a_2, a_3) = (s, y, (1-c(s)y)\tan\tilde{\theta}) \tag{3.9}$$

the ideal kinematic model is transformed into the general chained system (3.6) in which

$$\begin{cases} m_1 = \dfrac{v\cos\tilde{\theta}}{1-yc(s)} \\ m_2 = \dfrac{d}{dt}((1-yc(s))\tan\tilde{\theta}) \\ \quad = -vc(s)\sin\tilde{\theta}\tan\tilde{\theta} - v\dfrac{dc(s)}{ds}\dfrac{\cos\tilde{\theta}}{1-yc(s)}\tan\tilde{\theta}y \\ \quad + v\dfrac{1-yc(s)}{\cos^2\tilde{\theta}}\left(\dfrac{\tan\delta}{l} - c(s)\dfrac{\cos\tilde{\theta}}{1-yc(s)}\right) \end{cases} \tag{3.10}$$

Form (3.9)(3.10), the expression of the single-input linear system (3.8) can be obtained. In [11] the virtual control input m_3 is designed to be a PD-type controller

$$m_3 = -K_d a_3 - K_p a_2 \qquad (K_p, K_d) \in R^{+2} \tag{3.11}$$

which leads to

$$a_2'' + K_d a_2' + K_p a_2 = 0 \tag{3.12}$$

It is easy to prove that both the state a_2 and a_3 can converge to zero asymptotically by choosing K_d, K_p. Through inverse conversion, the physical control law is obtained as

$$\begin{aligned}\delta(y,\tilde{\theta}) \quad = \arctan\Bigg(l\Bigg[\frac{\cos^3\tilde{\theta}}{(1-yc(s))^2}\Big(\frac{dc(s)}{ds}y\tan\tilde{\theta} - K_d(1-yc(s))\tan\tilde{\theta} - K_p y \\ +c(s)(1-yc(s))\tan^2\tilde{\theta}\Big) + \frac{c(s)\cos\tilde{\theta}}{1-yc(s)}\Bigg]\Bigg)\end{aligned} \tag{3.13}$$

Satisfactory path following results have been reported in [11] provided the vehicles move without sliding.

But in actual applications especially when vehicles move on a slippery ground or make a turn on a slope, the substantial sliding effects cannot be ignored which causes a significant lateral deviation.

3.3 Robust control law design

In this section a sliding mode controller is designed based on the vehicle-oriented kinematic model (3.5) in which sliding effects are considered as additive disturbances.

3.3.1 Sliding mode control for perturbed chained system

[24] has designed a sliding mode controller to stabilize a nonholonomic perturbed systems, but all the disturbances have to satisfy a linear constraint. [25] has investigated the problem of designing robust controllers for general chained systems. A sliding mode controller was designed after the chained system was converted into a single-input and time-varying linear model by setting one input as a time-varying function, but unfortunately the system becomes no longer always controllable. To overcome this problem a new scheme is proposed in this section to design a sliding mode controller with the help of the natural algebraic structure of chained systems.

Considering the kinematic model (3.5), a perturbed chained system (3.14) can be obtained when the same coordinates transformation (3.9) is used,

$$\text{derivation w.r.t } \boldsymbol{t}\begin{cases}\dot{a}_1 = \dfrac{v\cos\tilde{\theta}}{1-yc(s)} = m_1 \\ \dot{a}_2 = v\sin\tilde{\theta} + \varepsilon_2 = a_3 m_1 + \varepsilon_2 \\ \dot{a}_3 = \dfrac{d}{dt}((1-yc(s))\tan\tilde{\theta}) \\ \quad\ = m_2 + \eta\end{cases} \tag{3.14}$$

where

$$\eta = \frac{(1-yc(s))\varepsilon_3}{\cos^2\tilde{\theta}} - c(s)\varepsilon_2\tan\tilde{\theta} \tag{3.15}$$

Noting that in (3.14) a_i and m_i have the same expression as it in (3.9-3.10), ε_2 and η act as two additive disturbances to the ideal system (3.6). So similarly (3.14) can be converted into a perturbed single-input linear system by computing the derivative with respect to the state variable a_1.

$$\text{derivation w.r.t } \boldsymbol{a}_1\begin{cases}a_1' = 1 \\ a_2' = a_3 + \dfrac{\varepsilon_2}{m_1} \\ a_3' = \dfrac{m_2}{m_1} + \dfrac{\eta}{m_1} = u + \dfrac{\eta}{m_1}\end{cases} \tag{3.16}$$

where u is the virtual control input of the disturbed single-input system (3.16). Remarking that u is velocity independent, $\frac{\varepsilon_2}{m_1}$ and $\frac{\eta}{m_1}$ are bounded. Because the single-input model (3.16) contains uncertain bounded disturbances, theories of sliding mode control are applied to design a robust controller which may guarantee the system states converge to a neighborhood of the origin.

Concerning the states a_2, a_3 for the path following problem, the sliding surface is defined as

$$z = \Lambda a_2 + a_3 \tag{3.17}$$

where $\Lambda > 0$. One condition that guarantees the system states reach the sliding manifold $z = 0$ is $z\dot{z} < 0$. Once the sliding manifold is encountered, the system stability is achieved.

Theorem 2: Define a strictly increasing function

$$s(t) = \int_0^t v^+(\tau)d\tau \tag{3.18}$$

where v^+ is positive definite and use the notation that $(\diamond)' = \dfrac{d\diamond}{ds}$, if the sign of $v^+(\tau)$ is kept positive, then the condition $zz' < 0$ is equivalent to the reaching condition $z\dot{z} < 0$.

Prove:

$$zz' = z\frac{dz}{ds} = z\frac{dz}{dt}\frac{dt}{ds} = z\dot{z}\frac{1}{v^+(\tau)} \tag{3.19}$$

if $zz' < 0$ then it is easy to prove that the reaching condition $z\dot{z} < 0$ is satisfied provided $v^+(\tau)$ is kept positive. □

In our applications, $s(t)$ is the curvilinear coordinates of point M, $v^+(\tau)$ is the linear velocity of point M along the desired path C. $v^+(\tau) = m_1$, since the orientation deviation $\tilde{\theta}$ of the vehicle with respect to the desired path C varies in the range of $(-\frac{\pi}{2}, \frac{\pi}{2})$ and the vehicle remains closed to the desired path which means that $1 - yc > 0$, from (3.10) the condition of $v^+(\tau) > 0$ is satisfied.

Theorem 3: Considering the system (3.14) where $(a_1, a_2, a_3) = \big(s, y, (1 - c(s)y)\tan\tilde{\theta}\big)$, define

$$z = \Lambda a_2 + a_3 = \Lambda y + (1 - yc(s))\tan\tilde{\theta} \tag{3.20}$$

the achievement of sliding motions on the sliding surface (3.20) can be guaranteed by the control law

$$u = -kz - \Lambda a_3 - \rho\text{sign}(z) \tag{3.21}$$

where

$$\rho \geq |\varsigma| = \Big|\frac{\Lambda\varepsilon_2 + \eta}{m_1}\Big| \tag{3.22}$$

Prove: For the states a_2, a_3, consider the reaching condition of sliding mode control:

$$\begin{aligned} zz' &= z(\Lambda a_2' + a_3') \\ &= z\Big(\Lambda a_3 + u + \frac{\Lambda\varepsilon_2 + \eta}{m_1}\Big) \\ &= z\Big(\Lambda a_3 + u + \varsigma\Big) \end{aligned} \tag{3.23}$$

Applying (3.21) into (3.23), we get

$$\begin{aligned} zz' &= z\Big(\Lambda a_3 - kz - \Lambda a_3 - \rho\text{sign}(z) + \varsigma\Big) \\ &< -kz^2 - (\rho - |\varsigma|)|z| \end{aligned} \tag{3.24}$$

if we choose ρ following (3.22), then the reaching condition $zz' < 0$ is satisfied guaranteeing a sliding motion on the sliding surface (3.20). On the sliding surface (3.20), one has

$$z = \Lambda a_2 + a_3 = 0 \tag{3.25}$$

which leads to

$$a_2' = -\Lambda a_2 + \frac{\varepsilon_2}{m_1} = -\Lambda a_2 + \varpi \tag{3.26}$$

The stability of system (3.26) has been analyzed in [21] in detail, from (3.26) a_2 can be expressed as

$$a_2 = e^{-\Lambda s}a_2(0) + \frac{\varpi}{\Lambda} = a_2(0)e^{-\Lambda\int_0^t v^+(\tau)d\tau} + \frac{\varpi}{\Lambda} \tag{3.27}$$

so the solutions of the resulting closed-loop system are globally uniformly ultimately bounded. □

3.3.2 Stability Analysis

Because of the condition $z = 0$, the following relationship can be obtained

$$\Lambda a_2 + a_3 = 0 \tag{3.28}$$

Due to the definition of a_2, a_3 in (3.9) and (3.16) , one get that

$$a_2' = y' = -\Lambda y + \nu \tag{3.29}$$

where $\nu = \frac{\varepsilon_2}{m_1}$. So it is proven that the lateral deviation y is globally uniformly ultimately bounded in the presence of sliding effects. Similarly the orientation error $\tilde{\theta}$ is proven uniformly ultimately bounded also.

3.3.3 Modified Sliding Mode Controller

Sliding mode control (3.21) is simple, robust and can guarantee transient performances, but the low level delay caused by hydraulic-driven steering systems always results in chattering responses which may wear down the actuator and excite unmodeled dynamics, possibly compromising performance and even stability. To mitigate the problem of chatter, the *signum* function is replaced by the hyperbolic tangent function $tanh()$

$$u = -kz - \Lambda a_3 - \rho \tanh(\frac{0.2785\rho z}{\sigma}) \quad \sigma > 0 \tag{3.30}$$

Combining (3.10) with (3.30), the physical steering angle is obtained by inverse conversion of the virtual robust control law u.

$$\delta(y, \tilde{\theta}) = \arctan\left(l\left[\frac{\cos^3\tilde{\theta}}{(1-yc(x))^2}\Big(\frac{dc(s)}{ds}y\tan\tilde{\theta} + u + c(s)(1-yc(s))\tan^2\tilde{\theta}\Big) + \frac{c(s)\cos\tilde{\theta}}{1-yc(s)}\right]\right) \tag{3.31}$$

Remarking that some constraints have to be added to the system to ensure the validity of the controller:

- Because of the definition of m_1 in (3.10) which requires $1 - yc(s) \neq 0$, the vehicle is not allowed to pass the curvature center of the path c, which means that $y < \frac{1}{c(s)}$ holds and makes the definition of ρ in (3.22) ture.
- Because of the definition of m_2 in (3.10) which requires $\cos\tilde{\theta} \neq 0$, the vehicle body axis cannot be vertical to the path, the orientation error varies only in the range of $(-\frac{\pi}{2}, \frac{\pi}{2})$.

However the importance of the constraints is limited due to the small path curvatures and the restricted range of the steering angle in most practical cases.

3.4 Simulation results

In this section, some simulation results are presented to validate the proposed control law. In order to fully demonstrate the effectiveness of the controller, two reference paths consisting of straight lines and curves are followed (see figure 3.2 and 3.5), the sliding effects are introduced to the system when the vehicle follows the desired path stepping into a curve. To simulate all the other external unconsidered disturbances, noises are always added to the system through the same channel as the control inputs. In the simulations, the gains used in the control law (3.21) are set as $\Lambda = 0.3$ $\rho = 0.08, k = 0.3$. To compare the control performances with the previous works, the control laws (3.13) are applied under the same condition except that we set the controller gains as $k_p = 0.09, k_d = 0.6$.

The simulation results of the lateral deviation for two path-following experiments are shown by figure 3.3 and 3.6 respectively, the results of the orientation errors are shown in figure 3.4 and 3.7. In the simulation results, the dashed line represents the results yielded by using the controller (3.13), the solid line depicts the results obtained by applying the sliding mode controller (3.31) proposed in this chapter.

Because the control law (3.13) does not take sliding effects into account and from theoretical point of view, the PD-type virtual control law is not robust against disturbances, it is clear that in figure (3.3) and (3.4)

it suffers from sliding greatly, when the sliding effects appear, its lateral deviation becomes more significant than the other. While the sliding mode control law proposed in this chapter provides satisfactory simulation results, it has good transient responses and is robust against not only the sliding effects but also other input noises which inevitably occur in actual applications, the simulation results show that the sliding effects affect both the lateral deviation and the orientation error weakly.

In figure(3.6) (3.7) although initial orientation errors lead to significant lateral deviations, the proposed robust controller still make both lateral deviation and orientation errors converge and stable around zero. But too much initial errors degrade the performance of robust controller by causing large overshoots in the starting stage. It is because that high gains of the robust controller yield too strong control signals which make the chattering effects worse than before.

3.5 Conclusion

The path following problem of autonomous agricultural vehicles in the presence of sliding is investigated in this chapter. A vehicle-oriented kinematic model which integrates the sliding effects as additive disturbances is used. From this model, a particular perturbed chained system is evolved. The use of the attractive structure of chained systems together with the sliding mode control leads to a robust controller which is robust to both the sliding effects and external disturbances. The system states have been theoretically proved globally uniformly ultimately bounded. The advantage of this new scheme is that

- The anti-sliding controller proposed in this chapter is developed still relying on chained system properties, so abundant linear system theories are available to design more powerful controllers without loss of nonlinear features.
- This scheme is a primary work of designing robust controllers for chained systems. Since chained systems have a perfect natural structure for the use of sliding mode control, some skillful high-dimensional sliding surfaces can be designed to fulfill more complicated tasks, for example longitudinal control or anti-sliding control of vehicles with four-wheel steering kinematic model.
- This scheme does not require more sensors and costs less on-board computation which yields a easy actual implementation.

Experimental comparative results with previous schemes show the effectiveness of the proposed control law.

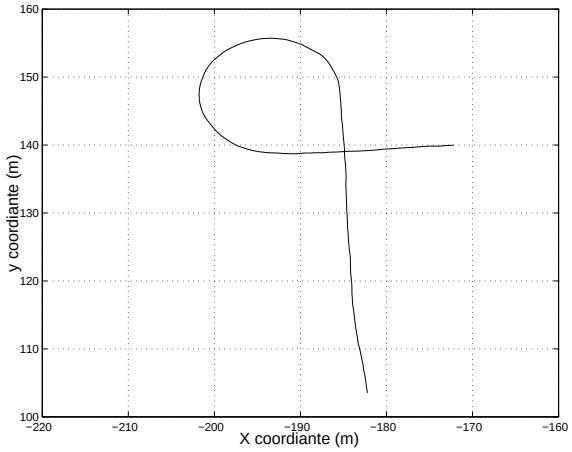

Figure 3.2: Path to be followed

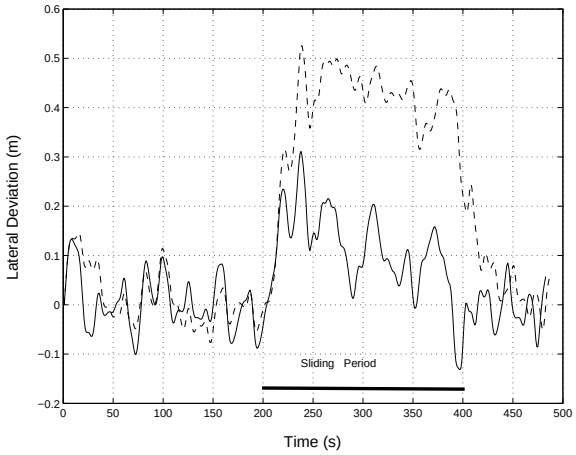

Figure 3.3: Lateral deviation

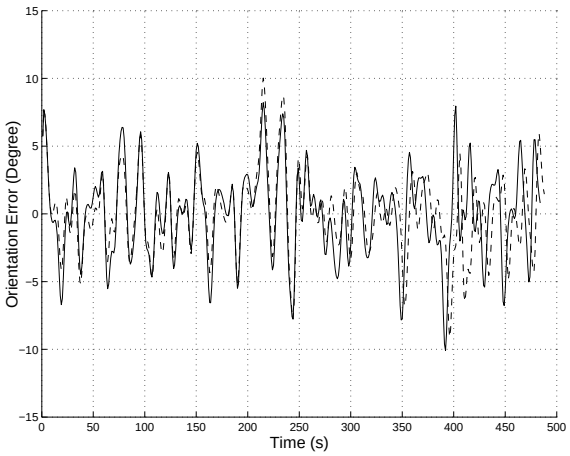

Figure 3.4: Orientation error

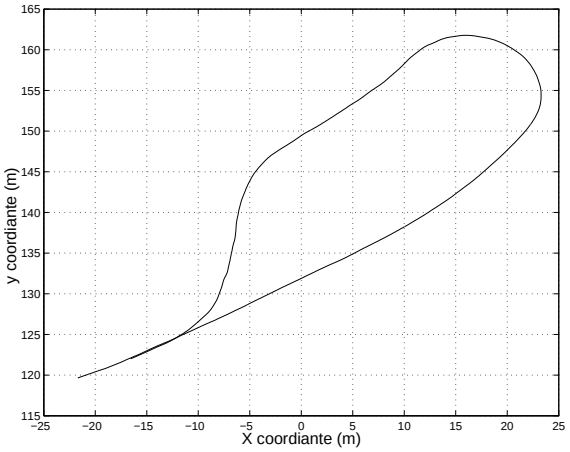

Figure 3.5: Path to be followed

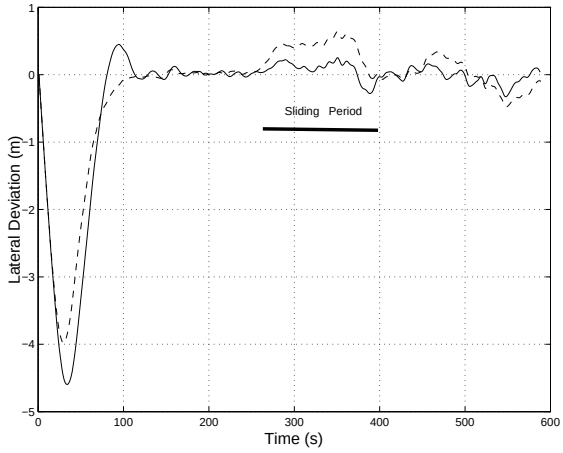

Figure 3.6: Lateral deviation

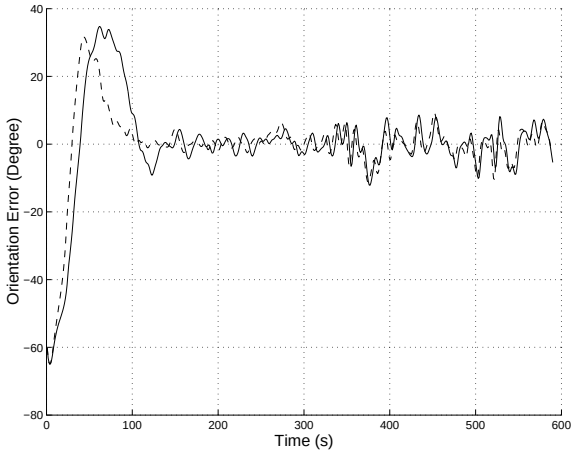

Figure 3.7: Orientation error

Chapter 4

ROBUST ADAPTIVE LATERAL CONTROL BY BACKSTEPPING

Most research works including chapter 3 treated sliding as disturbances which can be rejected by robust controllers. But as demonstrated in chapter 3, high-gain robust controllers are not realistic for autonomous vehicles with low-level delay, so another promising solution would be to develop low-gain controllers to share the undertaking of the robust controllers.

Alternatively sliding can be also regarded specifically as time-varying parameters. On the other hand backstepping methods which have been used widely in controller design are proven powerful in controlling nonholonomic systems with uncertain parameters [21][23], so the purpose in this chapter is to use backstepping methods to design a practical path following controller in presence of sliding with small control gains. The main idea of this chapter is to regard sliding effects as unknown parameters added to the ideal kinematic model. Based on *backstepping method* an adaptive controller is designed to estimate and compensate modeled time-invariant sliding components, furthermore two approaches are proposed to make the adaptive controller more robust to the time-varying sliding effects and noises. This chapter is organized as follows, in section 4.1 a vehicle-oriented kinematic model considering sliding is constructed in the path frame. In section 4.2 by assuming sliding is time-invariant, an adaptive controller is designed using backstepping methods. In section 4.3 robust adaptive controllers are obtained by integrating VSC or applying projection mapping. In section 4.4, some comparative simulation results are presented to validate the proposed control law.

4.1 Kinematic model

4.1.1 Notation and Problem Description

In this chapter the vehicle is simplified into a bicycle model. The kinematic model is expressed with respect to the path in frame (M, η_t, η_n), variables necessary in the kinematic model are denoted as follows: (see figure 4.1)

- C is the path to be followed.
- O is the center of the vehicle virtual rear wheel.
- M is the orthogonal projection of O on path C.
- η_t is the tangent vector to the path at M.
- η_n is the normal vector at M.
- y is the lateral deviation between O and M
- s is the curvilinear coordinates (arc-length) of point M along the path from an initial position.
- $c(s)$ is the curvature of the path at point M.

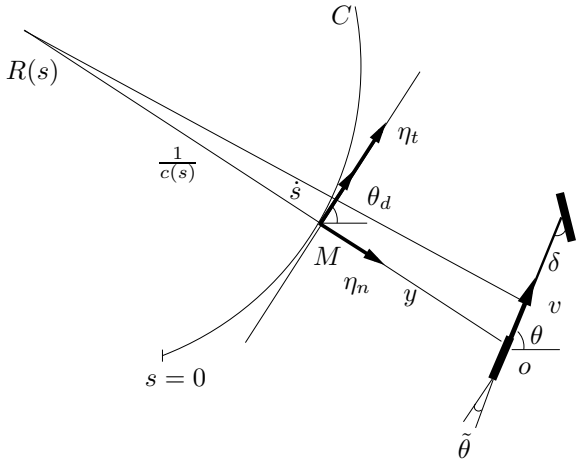

Figure 4.1: Notation and path frame description

- $\theta_d(s)$ is the orientation of the tangent to the path at point M with respect to the inertia frame.
- θ is the orientation of the vehicle centerline with respect to the inertia frame.
- $\tilde{\theta} = \theta - \theta_d$ is the orientation error.
- l is the vehicle wheelbase.
- v is the vehicle linear longitudinal velocity.
- δ is the steering angle of the virtual front wheel

So the vehicle movement can be described by $(y, s, \tilde{\theta})$. In this chapter path following control law

$$\delta = K(s, y, \tilde{\theta}, v) \tag{4.1}$$

will be designed to guarantee

$$\lim_{t\to\infty} y = 0 \tag{4.2}$$

and $\tilde{\theta}$ is bounded in presence of sliding.

4.1.2 Kinematic Model

In section 2.1.2, we have obtained a linearized kinematic model taking into account sliding

$$\begin{cases} \dot{s} = \dfrac{v\cos\tilde{\theta}}{1-c(s)y} - \dfrac{\psi(t)\sin\tilde{\theta}}{1-c(s)y} \\ \dot{y} = v\sin\tilde{\theta} + \psi(t)\cos\tilde{\theta} \\ \dot{\tilde{\theta}} = v\Big(\dfrac{\tan\delta}{l} - \dfrac{c(s)\cos\tilde{\theta}}{1-c(s)y}\Big) + \dfrac{v}{l}\eta(t) + \big(\dfrac{c(s)\sin\tilde{\theta}}{1-c(s)y} - \dfrac{1}{l}\big)\psi(t) \end{cases} \tag{4.3}$$

where $\psi(t) = v_y$ indicates the lateral sliding velocity, $\eta(t)$ is linked to the steering bias δ_b including inaccuracy due to linearization approximation. (see figure 4.2)

Since we only concern about lateral control, the reduced kinematic model for path following control is

$$\begin{cases} \dot{y} = v\sin\tilde{\theta} + \psi(t)\cos\tilde{\theta} \\ \dot{\tilde{\theta}} = v\Big(\dfrac{\tan\delta}{l} - \dfrac{c(s)\cos\tilde{\theta}}{1-c(s)y}\Big) + \dfrac{v}{l}\eta(t) + \big(\dfrac{c(s)\sin\tilde{\theta}}{1-c(s)y} - \dfrac{1}{l}\big)\psi(t) \end{cases} \tag{4.4}$$

4.2 Adaptive Control Law Design

In actual agriculture applications, farm vehicles always move with smooth velocities and most paths to be followed are straight lines and circles. The accelerations and the path curvature vary quite slowly with time, hence $\psi(t), \eta(t)$ can be approximated as

$$\begin{cases} \psi(t) = \psi_s + \breve{\psi}(t) \\ \eta(t) = \eta_s + \breve{\eta}(t) \end{cases} \tag{4.5}$$

where the sliding components ψ_s, η_s are almost time-invariant, $\breve{\psi}(t), \breve{\eta}(t)$ are time-varying variables. In this section by assuming $\dot{\psi}_s = \dot{\eta}_s = 0$ and $\breve{\psi}(t) = \breve{\eta}(t) = 0$, an adaptive controller will be designed. The inaccuracy of this approximation mainly consisting of trivial time-varying sliding effects is not important, it will be treated as disturbances and rejected by robust controller design in forthcoming section 4.3.

4.2.1 Backstepping-based Control Design Scheme

In the model (4.4), the lateral deviation y is not directly controlled. To overcome this problem the idea of backstepping is used; see [22] for details. Using backstepping we propose a stepwise control design procedure for this 2-order nonholonomic system with unknown parameters.

step 1: Consider the lateral subsystem of (4.4) and assumption of time-invariant sliding, the Lyapunov function candidate is chosen as

$$V_1 = \tfrac{1}{2}y^2 + \tfrac{1}{2}(\hat{\psi}_s - \psi_s)^T \Gamma^{-1} (\hat{\psi}_s - \psi_s) \tag{4.6}$$

where Γ is positive definite, $\hat{\psi}_s$ indicates the estimation of ψ_s. The time derivative of V_1 along the kinematic model is

$$\dot{V}_1 = y(v \sin\tilde{\theta} + \hat{\psi}_s \cos\tilde{\theta}) + (\hat{\psi}_s - \psi_s)^T \Gamma^{-1} (\dot{\hat{\psi}}_s - \Gamma y \cos\tilde{\theta}) \tag{4.7}$$

Regard $u_1 = \sin\tilde{\theta}$ as the virtual control input of the first step. If choose u_1 as

$$u_{1d} = \frac{-k_1 y - \hat{\psi}_s \cos\tilde{\theta}}{v} \tag{4.8}$$

and

$$\dot{\hat{\psi}}_s = \Gamma y \cos\tilde{\theta} \tag{4.9}$$

then we have

$$\dot{V}_1 = -k_1 y^2 \tag{4.10}$$

u_{1d} is the desired value of the virtual control input u_1 for the first step. If u_1 tracks (4.8) precisely, then the lateral subsystem of (4.4) can be stabilized asymptotically.

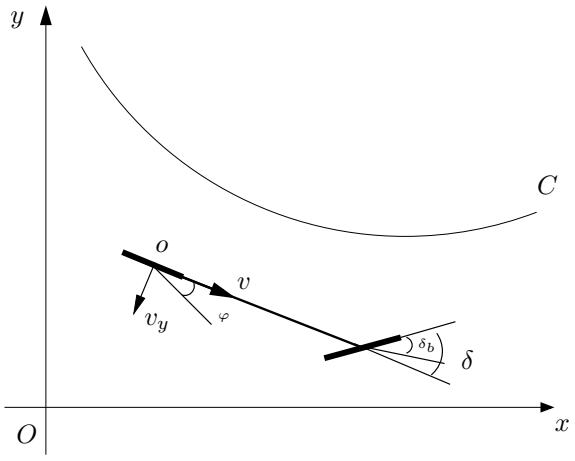

Figure 4.2: Notations of sliding effects

In the closed-loop system u_1 is not the actual control input, tracing u_{1d} with some errors indeed, so an error variable $\tilde{u}_1$ is defined as

$$\tilde{u}_1 = u_1 - u_{1d} \tag{4.11}$$

The time derivative of $\tilde{u}_1$ can be computed as

$$\begin{aligned}\dot{\tilde{u}}_1 &= \cos\tilde{\theta}\dot{\tilde{\theta}} + \frac{k_1\dot{y} + \dot{\hat{\psi}}_s\cos\tilde{\theta} - \hat{\psi}_s\sin\tilde{\theta}\dot{\tilde{\theta}}}{v} \\ &= m_1\Big(v\big(\frac{\tan\delta}{l} - \frac{c(s)\cos\tilde{\theta}}{1-c(s)y}\big) + m_3\eta_s + m_2\psi_s\Big) + \frac{\dot{\hat{\psi}}_s\cos\tilde{\theta} + k_1(v\sin\tilde{\theta} + \psi_s\cos\tilde{\theta})}{v}\end{aligned} \tag{4.12}$$

where

$$\begin{aligned}m_1 &= \cos\tilde{\theta} - \frac{\hat{\psi}_s\sin\tilde{\theta}}{v} \\ m_2 &= \frac{c(s)\sin\tilde{\theta}}{1-c(s)y} - \frac{1}{l} \\ m_3 &= \frac{v}{l}\end{aligned} \tag{4.13}$$

Note that

$$m_1 = \frac{1}{\cos\varphi}\cos(\tilde{\theta} + \varphi) \tag{4.14}$$

where φ is the slip angle defined in figure 4.2, so assuming $|\tilde{\theta} + \varphi| < \frac{\pi}{2}$, one get $m_1 > 0$.

Remark: For simplicity it is assumed that v is constant, in case v is time-varying, only variation is adding $\frac{(-k_1 y - \hat{\psi}_s\cos\tilde{\theta})\dot{v}}{v^2}$ in (4.12).

step 2: Considering the Lyapunov function as

$$V_2 = V_1 + \tfrac{1}{2}\tilde{u}_1^2 + \tfrac{1}{2}(\hat{\eta}_s - \eta_s)^T\gamma^{-1}(\hat{\eta}_s - \eta_s) \tag{4.15}$$

where γ is positive definite, $\hat{\eta}_s$ indicates the estimation of η_s. Regard $u_2 = \tan\delta$ as the virtual control input of the second step, then the time derivative of V_2 along (4.7)(4.12) is

$$\begin{aligned}\dot{V}_2 &= y(vu_1 + \hat{\psi}_s\cos\tilde{\theta}) + (\hat{\psi}_s - \psi_s)^T\Gamma^{-1}(\dot{\hat{\psi}}_s - \Gamma y\cos\tilde{\theta}) \\ &+\tilde{u}_1 m_1\big(v(\frac{u_2}{l} - \frac{c(s)\cos\tilde{\theta}}{1-c(s)y}) + m_3\eta_s + m_2\psi_s\big) \\ &+\tilde{u}_1\frac{k_1(v\sin\tilde{\theta} + \psi_s\cos\tilde{\theta}) + \dot{\hat{\psi}}_s\cos\tilde{\theta}}{v} + (\hat{\eta}_s - \eta_s)^T\gamma^{-1}\dot{\hat{\eta}}_s\end{aligned} \tag{4.16}$$

Substituting (4.8)(4.11) into (4.16), we have the following equation

$$\begin{aligned}\dot{V}_2 &= -k_1y^2 + yv\tilde{u}_1 + (\hat{\psi}_s - \psi_s)^T\Gamma^{-1}(\dot{\hat{\psi}}_s - \Gamma y\cos\tilde{\theta}) \\ &+\tilde{u}_1 m_1\big(v(\frac{u_2}{l} - \frac{c(s)\cos\tilde{\theta}}{1-c(s)y}) + m_3\eta_s + m_3\hat{\eta}_s - m_3\hat{\eta}_s + m_2\psi_s + m_2\hat{\psi}_s - m_2\hat{\psi}_s\big) \\ &+\tilde{u}_1\frac{k_1(v\sin\tilde{\theta} + \psi_s\cos\tilde{\theta} + \hat{\psi}_s\cos\tilde{\theta} - \hat{\psi}_s\cos\tilde{\theta}) + \dot{\hat{\psi}}_s\cos\tilde{\theta}}{v} + (\hat{\eta}_s - \eta_s)^T\gamma^{-1}\dot{\hat{\eta}}_s \\ &= -k_1y^2 + yv\tilde{u}_1 + (\hat{\psi}_s - \psi_s)^T\Gamma^{-1}(\dot{\hat{\psi}}_s - \Gamma y\cos\tilde{\theta}) \\ &+\tilde{u}_1 m_1\big(v(\frac{u_2}{l} - \frac{c(s)\cos\tilde{\theta}}{1-c(s)y}) + m_3\hat{\eta}_s + m_2\hat{\psi}_s\big) + \tilde{u}_1 m_1 m_3(\eta_s - \hat{\eta}_s) + \tilde{u}_1 m_1 m_2(\psi_s - \hat{\psi}_s) \\ &+\tilde{u}_1\frac{k_1(v\sin\tilde{\theta} + \hat{\psi}_s\cos\tilde{\theta}) + \dot{\hat{\psi}}_s\cos\tilde{\theta}}{v} + \tilde{u}_1\frac{k_1(\psi_s - \hat{\psi}_s)\cos\tilde{\theta}}{v} + (\hat{\eta}_s - \eta_s)^T\gamma^{-1}\dot{\hat{\eta}}_s \\ &= -k_1y^2 + \tilde{u}_1 m_1\big(v(\frac{u_2}{l} - \frac{c(s)\cos\tilde{\theta}}{1-c(s)y}) + m_3\hat{\eta}_s + m_2\hat{\psi}_s\big) \\ &+yv\tilde{u}_1 + \tilde{u}_1\frac{k_1(v\sin\tilde{\theta} + \hat{\psi}_s\cos\tilde{\theta}) + \dot{\hat{\psi}}_s\cos\tilde{\theta}}{v} \\ &+(\hat{\eta}_s - \eta_s)^T\gamma^{-1}(\dot{\hat{\eta}}_s - \tilde{u}_1\gamma m_1 m_3) \\ &+(\hat{\psi}_s - \psi_s)^T\Gamma^{-1}(\dot{\hat{\psi}}_s - \Gamma y\cos\tilde{\theta} - \Gamma k_1\frac{\tilde{u}_1\cos\tilde{\theta}}{v} - \Gamma\tilde{u}_1 m_1 m_2)\end{aligned} \tag{4.17}$$

In (4.17) let

$$\begin{aligned}\dot{\hat{\psi}}_s &= \Gamma y\cos\tilde{\theta} + \frac{\Gamma k_1\cos\tilde{\theta}}{v}\tilde{u}_1 + \Gamma\tilde{u}_1 m_1 m_2 \\ \dot{\hat{\eta}}_s &= \gamma m_1 m_3\tilde{u}_1\end{aligned} \tag{4.18}$$

and choose u_2 as

$$u_2 = l(-\frac{y}{m_1} - \frac{k_2\tilde{u}_1}{m_1 v} - \frac{m_3\hat{\eta}_s + m_2\hat{\psi}_s}{v} + \alpha + \beta) \tag{4.19}$$

where

$$\alpha = -\frac{k_1(v\sin\tilde{\theta} + \hat{\psi}_s\cos\tilde{\theta}) + \dot{\hat{\psi}}_s\cos\tilde{\theta}}{v^2 m_1} \tag{4.20}$$

$$\beta = \frac{c(s)\cos\tilde{\theta}}{1 - yc(s)} \tag{4.21}$$

then we get

$$\dot{V}_2 = -k_1 y^2 - k_2\tilde{u}_1^2 \tag{4.22}$$

Finally the vehicle steering angle δ is determined by

$$\delta = \arctan u_2 \tag{4.23}$$

4.2.2 Stability Analysis

From (4.22) it is known that the solutions $y, \tilde{u}_1$ and estimation errors $\tilde{\psi}_s, \tilde{\eta}_s$ are bounded on $[0, +\infty)$. The direct application of LaSalle invariance principle yields that all the solutions converge to the set Ω with

$$\Omega = \{(y, \tilde{u}_1, \hat{\psi}_s, \hat{\eta}_s) : y = 0, \tilde{u}_1 = 0\} \tag{4.24}$$

From (4.24), one gets that the lateral deviation will converge to zero asymptotically, simultaneously the steady orientation error $\tilde{\theta}$ is bounded by

$$\tan\tilde{\theta} = -\frac{\hat{\psi}_s}{v} \tag{4.25}$$

It is obvious that when vehicles move without sliding ($\hat{\psi}_s = 0$), the orientation error will converge to zero.

4.3 Robust Adaptive Controller Design

4.3.1 Kinematic Model with Time-varying Sliding

We have designed an adaptive controller when assuming that the sliding effects are time-invariant, but the precise kinematic model with sliding is

$$\begin{cases} \dot{y} = v\sin\tilde{\theta} + \psi_s\cos\tilde{\theta} + \varepsilon_1 \\ \dot{\tilde{\theta}} = v\Big(\dfrac{\tan\delta}{l} - \dfrac{c(s)\cos\tilde{\theta}}{1 - c(s)y}\Big) + m_3\eta_s + m_2\psi_s + \varepsilon_2 \end{cases} \tag{4.26}$$

where

$$\begin{aligned} \varepsilon_1 &= \breve{\psi}(t)\cos\tilde{\theta} + \varsigma_1 \\ \varepsilon_2 &= m_3\breve{\eta}(t) + m_2\breve{\psi}(t) + \varsigma_2 \end{aligned} \tag{4.27}$$

ς_1, ς_2 are unknown external disturbances. It is still an open problem to design controllers using backstepping algorithm for a system with time-varying parameters in presence of bounded disturbances and noise. In the latest literature [23] a new parametrization and filter structure that take into account parameter variation lead to a new backstepping controller when the time variation of the parameters is known. It is indicated that the uncertainty in the parameters can be counteracted by increasing the values of the design parameters. But high-gain controllers are not realistic for farm vehicles because of constrained control inputs and limited bandwidth of the steering systems.

The time-varying sliding components $\breve{\psi}(t), \breve{\eta}(t)$ have small amplitudes and we also assume that external disturbances are bounded, so it is reasonable to assume that $\varepsilon_1, \varepsilon_2$ are bounded

$$|\varepsilon_i| < \rho_i \tag{4.28}$$

Using the similar backstepping procedures, we can prove that

$$\dot{V}_1 = y(v\sin\tilde{\theta} + \hat{\psi}_s\cos\tilde{\theta}) + (\hat{\psi}_s - \psi_s)^T\Gamma^{-1}(\dot{\hat{\psi}}_s - \Gamma y\cos\tilde{\theta}) + y\varepsilon_1 \tag{4.29}$$

Still choose $\tilde{u}_{1d}$ as (4.8), then $\dot{\tilde{u}}_1$ becomes

$$\begin{aligned}\dot{\tilde{u}}_1 &= \cos\tilde{\theta}\dot{\tilde{\theta}} + \frac{k_1\dot{y} + \dot{\hat{\psi}}_s\cos\tilde{\theta} - \hat{\psi}_s\sin\tilde{\theta}\dot{\tilde{\theta}}}{v} \\ &= m_1\Big(v\big(\frac{\tan\delta}{l} - \frac{c(s)\cos\tilde{\theta}}{1-c(s)y}\big) + m_3\eta_s + m_2\psi_s + \varepsilon_2\Big) + \frac{\dot{\hat{\psi}}_s\cos\tilde{\theta} + k_1(v\sin\tilde{\theta} + \psi_s\cos\tilde{\theta} + \varepsilon_1)}{v}\end{aligned} \tag{4.30}$$

Substituting (4.29) and (4.30) into the derivative of V_2, moreover applying the resulting adaptive laws (4.18) and the controller (4.19), we can prove that

$$\dot{V}_2 = -k_1y^2 - k_2\tilde{u}_1^2 + y\varepsilon_1 + \tilde{u}_1(m_1\varepsilon_2 + \frac{k_1\varepsilon_1}{v}) \tag{4.31}$$

which implies that the closed-loop system is globally uniformly bounded.

4.3.2 Robust Adaptive Controller with Variable Structure Controller

Here we are in the place to design a controller which is robust to ε_i. Combining classical robust controllers with adaptive controllers is straightforward [28]. Considering the derivative of V_1 (4.29), in the first step if we choose

$$u_{1d} = \frac{-k_1y - \hat{\psi}_s\cos\tilde{\theta} - \rho_1 sign(y)}{v} \tag{4.32}$$

and the conditions $u_1 = u_{1d}$ and $\dot{\hat{\psi}}_s = \Gamma y\cos\tilde{\theta}$ are hold, then we can obtain

$$\dot{V}_1 < -k_1y^2 - |y|(\rho_1 - |\varepsilon_1|) \tag{4.33}$$

which yields the lateral deviation converges to zero.

Since $sign(\cdot)$ is not differentiable, in this section $sign(\cdot)$ is replaced by $\tanh(\cdot)$ which is continuously differentiable in the stepwise procedures to design robust controllers. Following the similar stepwise procedures as section 4.2.1, in the first step we choose

$$u_{1d} = \frac{-k_1y - \hat{\psi}_s\cos\tilde{\theta} - \rho_1\tanh(\frac{y}{\sigma_3})}{v} \tag{4.34}$$

so the derivative of $\tilde{u}_1$ is

$$\begin{aligned}\dot{\tilde{u}}_1 &= \cos\tilde{\theta}\dot{\tilde{\theta}} + \frac{k_1\dot{y} + \dot{\hat{\psi}}_s\cos\tilde{\theta} - \hat{\psi}_s\sin\tilde{\theta}\dot{\tilde{\theta}} + \frac{d\big[\rho_1\tanh(\frac{y}{\sigma_3})\big]}{dt}}{v} \\ &= m_1\Big(v\big(\frac{\tan\delta}{l} - \frac{c(s)\cos\tilde{\theta}}{1-c(s)y}\big) + m_3\eta_s + m_2\psi_s + \varepsilon_2\Big) + \frac{1}{v}\Big[\dot{\hat{\psi}}_s\cos\tilde{\theta} + \big[k_1 + \big(1-\tanh^2(\frac{y}{\sigma_3})\big)\frac{\rho_1}{\sigma_3}\big]\dot{y}\Big]\end{aligned} \tag{4.35}$$

Substituting (4.33) (4.34) and (4.35) into the derivative of V_2, following the similar developing procedures as section 4.2.1, finally we have the following equation

$$\begin{aligned}&\dot{V}_2 < -k_1y^2 - (\rho_1 - |\varepsilon_1|)|y| + \tilde{u}_1m_1\big(v(\frac{1}{l}u_2 - \frac{c(s)\cos\tilde{\theta}}{1-c(s)y}) + m_3\hat{\eta}_s + m_2\hat{\psi}_s + \varepsilon_2\big) \\ &+yv\tilde{u}_1 + \tilde{u}_1\frac{\varpi(v\sin\tilde{\theta} + \hat{\psi}_s\cos\tilde{\theta}) + \dot{\hat{\psi}}_s\cos\tilde{\theta}}{v} + \frac{1}{v}\tilde{u}_1\varpi\varepsilon_1 \\ &+(\hat{\eta}_s - \eta_s)^T\gamma^{-1}(\dot{\hat{\eta}}_s - \tilde{u}_1\gamma m_1m_3) \\ &+(\hat{\psi}_s - \psi_s)^T\Gamma^{-1}(\dot{\hat{\psi}}_s - \Gamma y\cos\tilde{\theta} - \Gamma\varpi\frac{\tilde{u}_1\cos\tilde{\theta}}{v} - \Gamma\tilde{u}_1m_1m_2) + \varsigma_1\end{aligned} \tag{4.36}$$

where

$$\varpi = k_1 + \big(1-\tanh^2(\frac{y}{\sigma_3})\big)\frac{\rho_1}{\sigma_3} \tag{4.37}$$

Then we can design a robust adaptive controller

$$u_2 = l(-\frac{y}{m_1} - \frac{k_2\tilde{u}_1}{m_1 v} - \frac{m_3\hat{\eta}_s + m_2\hat{\psi}_s}{v} + \alpha + \beta + s_1 + s_2) \tag{4.38}$$

where β, $\dot{\hat{\eta}}_s$ are defined as before and

$$\begin{aligned}
\alpha &= -\frac{\varpi(v\sin\tilde{\theta} + \hat{\psi}_s\cos\tilde{\theta}) + \dot{\hat{\psi}}_s\cos\tilde{\theta}}{v^2 m_1} \\
s_1 &= -\frac{\rho_1\varpi}{v^2 m_1}\tanh(\frac{\tilde{u}_1}{\sigma_1}) \\
s_2 &= -\frac{\rho_2}{v}\tanh(\frac{\tilde{u}_1}{\sigma_2}) \\
\dot{\hat{\psi}}_s &= \Gamma y\cos\tilde{\theta} + \frac{\Gamma\varpi\cos\tilde{\theta}}{v}\tilde{u}_1 + \Gamma\tilde{u}_1 m_1 m_2
\end{aligned} \tag{4.39}$$

where $\sigma_i > 0$. In this controller s_1 is developed to reject ε_1 appearing in the derivative of $\tilde{u}_1$, s_2 is to reject ε_2 in $\dot{\tilde{\theta}}$. The controller (4.38) leads to

$$\dot{V}_2 < -k_1 y^2 - k_2\tilde{u}_1^2 - (\rho_1 - |\varepsilon_1|)|y| - m_1|\tilde{u}_1|(\rho_2 - |\varepsilon_2|) - \frac{\varpi}{v}|\tilde{u}_1|(\rho_1 - |\varepsilon_1|) + \varsigma_2 \tag{4.40}$$

ς_i is trivial errors due to the substitution of $sign()$ by $tanh()$. So the robust adaptive controller (4.38) and adaptive laws (4.39) can guarantee the closed-loop system stable.

4.3.3 Projection Mapping for Parameter Adaptation

Another approach to design robust adaptive controllers is utilizing projection mapping for the parameter adaptation procedures. The projection mapping $Proj_\xi(\bullet)$ is defined by [29, 30]

$$Proj_\xi(\bullet) = \begin{cases} 0 & if \ \ \hat{\xi} = \xi_{\max} \ \ and \ \ \bullet > 0 \\ 0 & if \ \ \hat{\xi} = \xi_{\min} \ \ and \ \ \bullet < 0 \\ \bullet & otherwise \end{cases} \tag{4.41}$$

By using projection mapping $Proj_\xi(\bullet)$, the robust adaptive laws become

$$\dot{\hat{\psi}}_s = Proj_{\psi_s}\big(\Gamma[\cos\tilde{\theta} \ \ \frac{k_1\cos\tilde{\theta}}{v} + m_1 m_2][y \ \tilde{u}_1]^T\big) \tag{4.42}$$

$$\dot{\hat{\eta}}_s = Proj_{\eta_s}\big(\gamma m_1 m_3\tilde{u}_1\big) \tag{4.43}$$

The system will converge into a neighborhood of zero. The prior information on the bounds of the sliding effects ψ_s, η_s can be obtained off-line after performing large number of absolute coordinates measurements under different typical working conditions.

4.4 Simulation Results

First a classical "U" path with a perfect circular arc (path #1) is followed to test the adaptive controller. In the simulations, the gains used in (4.18), (4.19-4.20) are set as $k_1 = 0.15$, $k_2 = 1.14$, $\Gamma = 0.15$, $\gamma = 0.02$. In actual implementations, the gains should be tuned gradually to make an optimal compromise between transient characteristic and limited bandwidth of the steering system. The constant sliding is introduced with $v_y = -0.1$, $\delta_b = -0.048$. The control law of our previous work (3.13) is applied also with the controller gains $k_p = 0.09, k_d = 0.6$. Because this control law does not take sliding effects into account, in figure 4.3 when the sliding appears the lateral deviation (dashed line) becomes significant. While the controller (4.19) can compensate sliding effects through estimating them on line, the lateral deviation (solid line) converges to zero with small offsets (due to linearization approximation in (4.4)) after deviating from the desired path. Since small control gains are used, the vehicle movements are kept smooth. The remarkable overshoots at the beginning and end of the curve are caused by "jump change" of the sliding effects and low level delay. The robust adaptive controller with VSC (4.38) is simulated also. Because the modeling inaccuracy

is counteracted by VSC, the lateral deviation can converge to zero with a good transient response (dotted line in figure 4.3). The bounded orientation errors are shown by figure 4.4. As analyzed by section 4.2.2 the orientation errors do not converge to zero, indeed they are bounded by (4.25), it is normal when sliding occurs known as "crab sliding". The evolution of the sliding parameters ψ (solid line), η (dashed line) is shown by figure 4.5. It is clear that at the beginning and end of the circle, $\hat{\psi}$ varies greatly which explains the overshoots of the lateral deviation, but as the vehicle follows the circle, $\hat{\psi}$,$\hat{\eta}$ evolve smoothly close to the real values. To simulate the actual working condition, a set of real measurement data is used in the simulation to reconstruct the actual v_y and δ_b. In figure 4.6 the adaptive controllers yield small lateral deviation with zero mean value, while the lateral deviation of the controller (3.13) is significant and has obvious bias.

In order to compare the performances between the robust controllers (4.38) and projection mappings (4.42-4.43), another reference path #2 consisting of straight lines and curves is followed (see figure 4.7), the lateral deviation is shown by figure 4.8. The experimental data indicates that the robust controller with VSC yields better transient performances at the expense of non-smooth movements (dotted line) especially when low level delay is considered. While the controller with projection mapping yields a movement with less oscillation following the reference path (solid line). So for the vehicles with good low-level characters, the controller with VSC is favorable, but for the vehicles whose bandwidth is limited, the robust controller with projection mapping is preferred.

4.5 Conclusion

The path following problem of autonomous agricultural vehicles in the presence of sliding is investigated in this chapter. A vehicle-oriented kinematic model which integrates the sliding effects as additive unknown parameters is constructed. From this model, a practical adaptive controller is designed based on the back-stepping method which can stabilize the lateral derivation near zero and guarantees the orientation error converge into a neighborhood near the origin. In addition two approaches are proposed to refine the adaptive controller, allowing it to be robust to the time-varying sliding components and external disturbances. Experimental comparative results show the effectiveness of the proposed control laws. The advantages of this scheme are that

- When no sliding occurs, it provides a path following controller which can guarantee lateral deviation and orientation error converge to zero.
- Instead of using high gains or powerful functions to counteract sliding effects, small controller gains are used to stabilize the system and the sliding effects are estimated by parameter adaptation, yielding precision path following with less oscillation.
- Backstepping procedures are used to design a path-following controller for a 2-order nonholonomic system, it can be extended to high order nonholonomic systems.

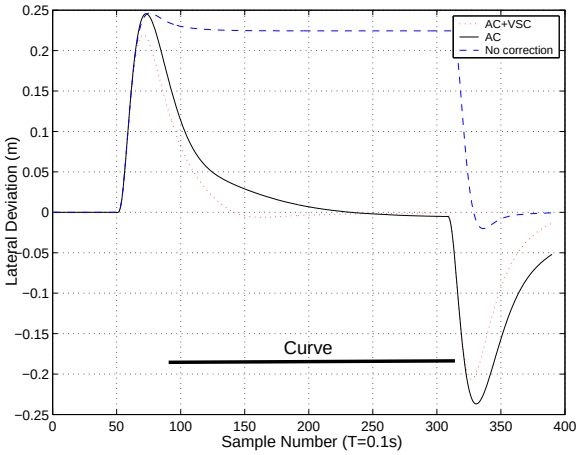

Figure 4.3: Lateral deviation of path #1

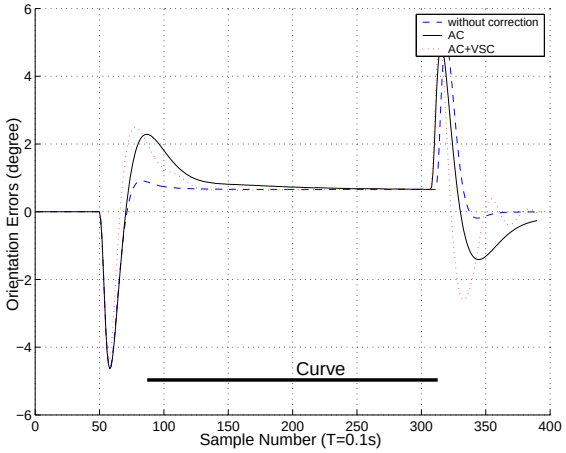

Figure 4.4: Orientation errors of path #1

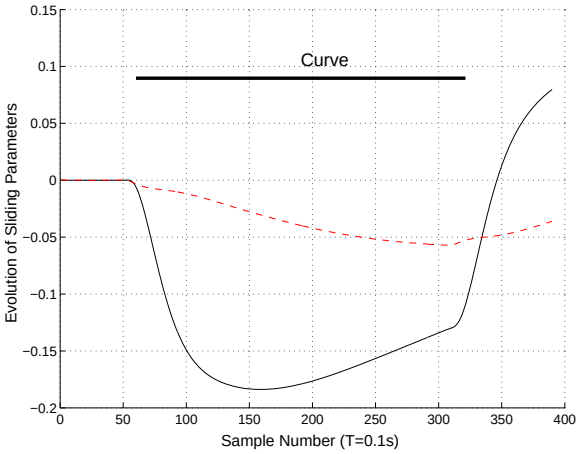

Figure 4.5: Evolution of sliding parameters

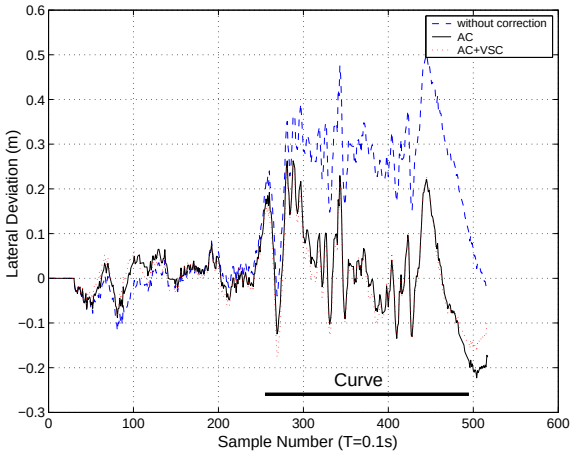

Figure 4.6: Lateral deviation of path #1 with real measurements

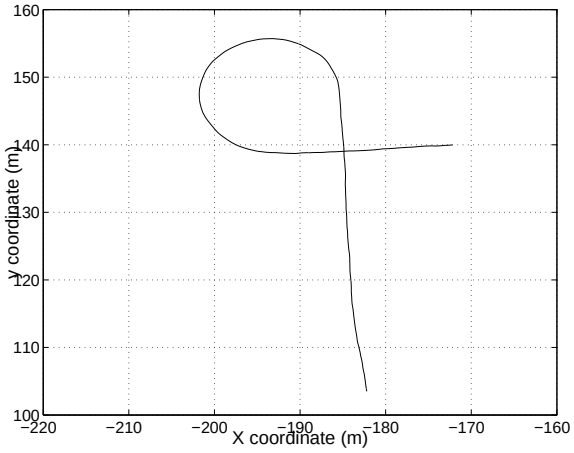

Figure 4.7: Path #2 to be followed

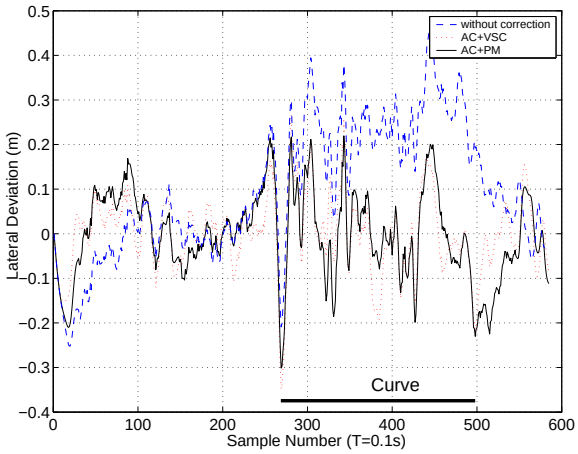

Figure 4.8: Lateral deviation of path #2 with real measurements

Chapter 5

TRAJECTORY TRACKING CONTROL IN PRESENCE OF SLIDING

In agriculture fields it is quite common that several vehicles (including cropping, threshing, cleaning, seeding and spraying machines) compose a platoon for combined harvesting. In this case driving safety requiring constant longitudinal distances between the leading vehicle and following vehicles is an additional requirement along with the effort of improving lateral path-following performances. Therefore vehicle motions are specified not only by a geometric path but also by a time law with respect to the longitudinal motions. Since longitudinal-lateral control becomes more and more important, many research teams have paid their attention to trajectory tracking control, satisfactory results have been reported as soon as vehicles satisfy pure rolling constraints [1], [3]-[6]. But as explained in last chapters, due to complex factors between tires and grounds the pure rolling constraints are never satisfied strictly especially for agriculture applications.

In chapter 4 we have applied backstepping successfully to design a path following controller, so the purpose of this chapter is to extend our lateral controller to design a practical longitudinal-lateral controller in presence of sliding. The main idea of this chapter is that sliding effects are introduced as additive unknown parameters to the ideal kinematic model, based on *backstepping method* a robust adaptive controller is designed. Moreover to be of benefit to actual applications the robust adaptive controller is simplified into an adaptive controller with projection mapping. This chapter is organized as follows, in section 5.1 a kinematic model considering sliding is constructed in the vehicle body frame. In section 5.2 a robust adaptive controller is designed by using backstepping methods. In section 5.3 the robust adaptive controller is simplified into an adaptive controller with projection mapping. In section 5.4 some comparative simulation results are presented to validate the proposed control laws.

5.1 Kinematic Model for Trajectory Tracking Control

5.1.1 Notation and Problem Description

In this chapter the vehicle is simplified into a bicycle model, the kinematic model is expressed in the vehicle body frame (o, x', y') (see figure 5.1). Variables necessary in the kinematic model are denoted as follows:

- o (o_r) is the center of the (reference) vehicle virtual rear wheel.
- x' is the vector corresponding to the vehicle body axis
- y' is the vector vertical to x'
- (x_r, y_r) are the coordinates of the reference vehicle o_r with respect to the inertia frame.
- (x, y) are the coordinates of the vehicle o with respect to the inertia frame.
- (x_e, y_e) are the coordinates of the vector $\overrightarrow{oo_r}$ in the frame (o, x', y')

- $c(s)$ is the curvature of the path, s is the curvilinear coordinates (arc-length) of the point o_r along the reference path from an initial position.
- θ (θ_r) is the orientation of the (reference) vehicle centerline with respect to the inertia frame.
- $\theta_e = \theta_r - \theta$ is the orientation error.
- l is the vehicle wheelbase.
- v (v_r) is the linear velocity of the (reference) vehicle with respect to the inertia frame.
- v_x is the longitudinal velocity of the vehicle in the direction of ox' in the inertia frame. In this chapter we assume that only lateral sliding occurs between tires and grounds, so v_x always equals to the wheel rotating velocity V_ω.
- δ is the steering angle of the virtual front wheel

So the trajectory tracking errors can be described by (x_e, y_e, θ_e). The aim of this chapter is to design a controller (v_x, δ) which can guarantee the longitudinal-lateral errors x_e, y_e approach to zero and the orientation error θ_e is bounded in presence of sliding.

5.1.2 Kinematic Model

From figure 5.1, it is easy to obtain the following geometric relationship

$$\begin{pmatrix} x_e \\ y_e \\ \theta_e \end{pmatrix} = \begin{pmatrix} \cos\theta & \sin\theta & 0 \\ -\sin\theta & \cos\theta & 0 \\ 0 & 0 & 1 \end{pmatrix} \begin{pmatrix} x_r - x \\ y_r - y \\ \theta_r - \theta \end{pmatrix} \tag{5.1}$$

In this chapter it is assumed that $|\theta_e| < \frac{\pi}{2}$. When vehicles move without sliding, the angular velocity can be expressed by

$$\dot{\theta} = \omega = \frac{v}{l}\tan\delta \tag{5.2}$$

The angular velocity of the reference vehicle is

$$\dot{\theta}_r = \frac{v_r}{\frac{1}{c(s)}} \tag{5.3}$$

The ideal kinematic model with respect to (o, x', y') can be developed directly by differentiating (5.1)

$$\begin{cases} \dot{x}_e = -v + v_r\cos\theta_e + \omega y_e \\ \dot{y}_e = v_r\sin\theta_e - \omega x_e \\ \dot{\theta}_e = v_r c(s) - \dfrac{v}{l}\tan\delta \end{cases} \tag{5.4}$$

But when vehicles move on a steep slope or the ground is slippery, sliding occurs inevitably, (5.4) is no longer valid. Since the longitudinal tire sliding is neglected, the violation of the pure rolling constraints is described by introducing the lateral sliding velocity v_y and bias of the steering angle δ_b. Therefore the velocity constraints become

$$\begin{cases} \dot{x} = v\cos(\theta + \varphi) \\ \dot{y} = v\sin(\theta + \varphi) \end{cases} \tag{5.5}$$

where

$$v = \sqrt{v_x^2 + v_y^2} \tag{5.6}$$

and φ is the side sliding angle defined by

$$\varphi = \arctan(\frac{v_y}{v_x}) \tag{5.7}$$

By using the similar method the kinematic model when sliding is taken into account is obtained

$$\begin{cases} \dot{x}_e = -v_x + v_r \cos\theta_e + \omega y_e \\ \dot{y}_e = -v_y + v_r \sin\theta_e - \omega x_e \\ \dot{\theta}_e = v_r c(s) - (\dfrac{v_x}{l}\tan(\delta + \delta_b) - \dfrac{v_y}{l}) \end{cases} \tag{5.8}$$

Remark that

$$v_x = v\cos\varphi \tag{5.9}$$

equals to the wheel rotating velocity which is the control law to be designed. In case no sliding occurs, $v_x = v$.

5.1.3 Kinematic Model with Linearization Approximation

In actual agriculture applications farm vehicles always move smoothly and most trajectories to be tracked are straight lines and circles without abrupt change of curvature, so the lateral sliding velocity and the steering bias vary not too greatly with time. Hence the sliding effects can be described exactly by

$$\begin{aligned} v_y &= \bar{v}_y + \varepsilon_1 \\ \delta_b &= \bar{\delta}_b + \varepsilon_2' \end{aligned} \tag{5.10}$$

where $\bar{v}_y$, $\bar{\delta}_b$ are time-invariant, ε_1, ε_2' are time-varying variables with zero mean value. Furthermore since the steering bias δ_b is quite small, the orientation kinematic equation in (5.8) can be linearized resulting in trivial errors. Therefore the kinematic model (5.8) is rewritten as

$$\dot{x}_e = -v_x + v_r\cos\theta_e + \omega y_e \tag{5.11a}$$

$$\dot{y}_e = v_r\sin\theta_e - \omega x_e - (\bar{v}_y + \varepsilon_1) \tag{5.11b}$$

$$\dot{\theta}_e = c(s)v_r - \frac{v_x}{l}\tan\delta + \frac{\bar{v}_y + \varepsilon_1}{l} - \frac{v_x}{l}(\tan\bar{\delta}_b + \varepsilon_2) \tag{5.11c}$$

where $\varepsilon_2 = \tan\varepsilon_2' + \epsilon$, ϵ is the error due to linearization approximation.

5.2 Backstepping-based Robust Adaptive Control Design

5.2.1 Trajectory Tracking Control for Ideal Kinematic Model

First the ideal kinematic model (5.4) is considered. Notice that (5.4) is a 2-3 nonholonomic system in which y_e is not directly controlled. To overcome this problem the idea of backstepping is used: see [22] for details. Using backstepping we propose a stepwise design procedure for this 3-order nonholonomic system.

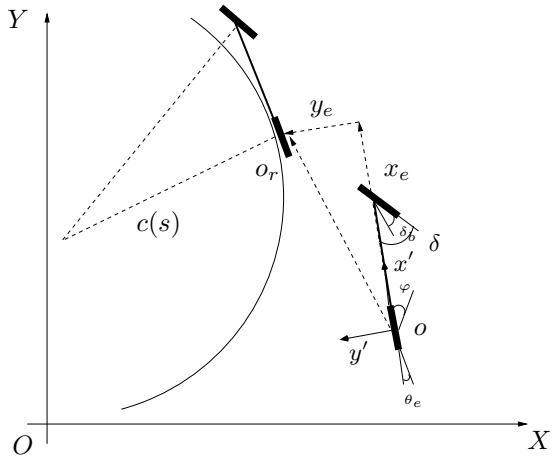

Figure 5.1: Notations of the kinematic model

Step 1 : Considering the ideal kinematic model (5.4), we choose the Lyapunov function candidate as

$$V_1 = \frac{1}{2}x_e^2 + \frac{1}{2}y_e^2 \tag{5.12}$$

The derivative of V_1 along (5.4) is

$$\dot{V}_1 = x_e(-v_x + v_r\cos\theta_e) + y_e(v_r\sin\theta_e) \tag{5.13}$$

Regard $u_1 = \sin\theta_e$ as the virtual control input of the first step. If choose u_1 as

$$u_{1d} = \frac{-k_y y_e}{v_r} \tag{5.14}$$

and choose the longitudinal velocity as

$$v_x = v_r\cos\theta_e + k_x x_e \tag{5.15}$$

then we have

$$\dot{V}_1 = -k_x x_e^2 - k_y y_e^2 \tag{5.16}$$

So u_{1d} of (5.14) is the desired value of the virtual control input u_1 for the first step. If u_1 tracks (5.14) precisely, then the longitudinal and lateral deviations will converge to zero asymptotically.

Indeed in the closed loop system u_1 is not the actual control input, tracking u_{1d} with some errors, therefore $\tilde{u}_1$ is defined as

$$\tilde{u}_1 = u_1 - u_{1d} \tag{5.17}$$

Computing the time derivative of $\tilde{u}_1$ yields to

$$\dot{\tilde{u}}_1 = \cos\theta_e\big(c(s)v_r - \frac{v_x}{l}\tan\delta\big) + \frac{k_y}{v_r}(v_r\sin\theta_e - \omega x_e) \tag{5.18}$$

step 2: Consider the Lyapunov function as

$$V_2 = V_1 + \frac{1}{2}\tilde{u}_1^2 \tag{5.19}$$

Then the time derivative of V_2 along (5.13) and (5.18) is

$$\dot{V}_2 = x_e(-v_x + v_r\cos\theta_e) + y_e v_r u_1 + \tilde{u}_1(\cos\theta_e v_r c(s) - (\cos\theta_e + \frac{k_y x_e}{v_r})\omega + k_y\sin\theta_e) \tag{5.20}$$

after substituting (5.14) (5.15) and (5.17) into (5.20), the following equation can be deduced

$$\dot{V}_2 = -k_x x_e^2 - k_y y_e^2 + \tilde{u}_1(y_e v_r + \cos\theta_e v_r c(s) - (\cos\theta_e + \frac{k_y x_e}{v_r})\omega + k_y\sin\theta_e) \tag{5.21}$$

In (5.21) if ω is chosen as

$$\omega = \frac{y_e v_r + \cos\theta_e v_r c(s) + k_y\sin\theta_e + k_u\tilde{u}_1}{\cos\theta_e + \frac{k_y x_e}{v_r}} \tag{5.22}$$

where

$$\tilde{u}_1 = \sin\theta_e + \frac{k_y y_e}{v_r} \tag{5.23}$$

Then we can obtain

$$\dot{V}_2 = -k_x x_e^2 - k_y y_e^2 - k_u\tilde{u}_1^2 \tag{5.24}$$

The resulting control laws are

$$\begin{aligned} v_x &= v_r\cos\theta_e + k_x x_e \\ \delta &= \arctan(\frac{l\omega}{v_x}) \end{aligned} \tag{5.25}$$

5.2.2 Stability Analysis

(5.24) leads to the stability of the closed-loop system. The direct application of LaSalle invariance principle yields that all the solutions converge to the set Ω with

$$\Omega = \{(x_e, y_e, \tilde{u}_1) : x_e = 0, y_e = 0, \tilde{u}_1 = 0\} \tag{5.26}$$

Moreover from (5.17), one gets that when the lateral deviation converges to zero, simultaneously the steady orientation error θ_e converges to zero also. So when vehicles move without sliding, the proposed controller can stabilize the closed-loop system to zero.

5.2.3 Robust Adaptive Control for Kinematic Model with Sliding

Consider the kinematic model with sliding (5.11). It is a 2-3 nonholonomic system with unknown constant parameters $\bar{v}_y$, $\bar{\delta}_b$ and time-varying disturbances ε_i. In this chapter it is assumed that ε_i is bounded by

$$|\varepsilon_i| < \rho_i \tag{5.27}$$

So we are in the place to design a controller which not only can estimate and compensate unknown parameters but also is robust to ε_i. To solve this problem a robust adaptive controller will be designed by combining backstepping schemes with Variable Structure control (VSC).

step 1: Consider the sub-kinematic equations (5.11a) and (5.11b). The Lyapunov function candidate is chosen as

$$V_1 = \frac{1}{2}x_e^2 + \frac{1}{2}y_e^2 + \frac{1}{2}(\hat{v}_y - \bar{v}_y)^T\Gamma^{-1}(\hat{v}_y - \bar{v}_y) \tag{5.28}$$

where Γ is positive definite, $\hat{v}_y$ indicates the estimation of $\bar{v}_y$. The time derivative of V_1 along the kinematic model is

$$\dot{V}_1 = x_e(-v_x + v_r\cos\theta_e) + y_e(v_r\sin\theta_e - \hat{v}_y - \varepsilon_1) + (\hat{v}_y - \bar{v}_y)^T\Gamma^{-1}(\dot{\hat{v}}_y + \Gamma y_e) \tag{5.29}$$

Regard $u_1 = \sin\theta_e$ as the virtual control input of the first step. If choose u_1 as a variable structure controller

$$u_{1d} = \frac{-k_y y_e + \hat{v}_y - \rho_1 sign(y_e)}{v_r} \tag{5.30}$$

and let

$$v_x = v_r\cos\theta_e + k_x x_e \tag{5.31}$$

$$\dot{\hat{v}}_y = -\Gamma y_e \tag{5.32}$$

then we have

$$\dot{V}_1 < -k_x x_e^2 - k_y y_e^2 - (\rho_1 - |\varepsilon_1|)|y_e| \tag{5.33}$$

So u_{1d} of (5.30) is the desired value of the virtual control input u_1 for the first step. If u_1 tracks (5.30) precisely, then the longitudinal and lateral deviations will converge to zero asymptotically.

Indeed in the closed loop system u_1 is not the actual control input, tracking u_{1d} with some errors, therefore $\tilde{u}_1$ is defined as

$$\tilde{u}_1 = u_1 - u_{1d} \tag{5.34}$$

In backstepping schemes the derivative of u_{1d} must appear in the following steps, but $sign()$ included in (5.30) is not differentiable, so $sign()$ is replaced by tanh() which is continuously differentiable. Therefore u_{1d} becomes

$$u_{1d} = \frac{-k_y y_e + \hat{v}_y - \rho_1\tanh(\dfrac{y_e}{\sigma_1})}{v_r} \tag{5.35}$$

where $\sigma_1 > 0$. Substituting (5.35) into (5.34) and computing the time derivative yield to

$$\dot{\tilde{u}}_1 = \cos\theta_e\big(c(s)v_r - \frac{v_x}{l}\tan\delta + \frac{\bar{v}_y + \varepsilon_1}{l} - \frac{v_x}{l}(\eta + \varepsilon_2)\big) + \frac{1}{v_r}(\varpi\dot{y}_e - \dot{\hat{v}}_y) \tag{5.36}$$

where

$$\eta = \tan\bar{\delta}_b \tag{5.37}$$

$$\varpi = k_y + \big(1 - \tanh^2(\frac{y_e}{\sigma_1})\big)\frac{\rho_1}{\sigma_1} \tag{5.38}$$

Remark: For simplicity it is assumed that v_r is constant, in case v_r is time-varying, only variation is adding $\frac{\dot{v}_r}{v_r^2}\big(-k_y y_e + \hat{v}_y - \rho_1 \tanh\frac{y_e}{\sigma_1}\big)$ in (5.36).

step 2: consider the Lyapunov function as

$$V_2 = V_1 + \frac{1}{2}\tilde{u}_1^2 + \frac{1}{2}(\hat{\eta}-\eta)^T\gamma^{-1}(\hat{\eta}-\eta) \tag{5.39}$$

where γ is positive definite, $\hat{\eta}$ indicates the estimation of η. Regard $u_2 = \tan\delta$ as the virtual control input of the second step, then the time derivative of V_2 along (5.29) is

$$\dot{V}_2 = x_e(-v_x + v_r\cos\theta_e) + y_e(v_r u_1 - \hat{v}_y - \varepsilon_1) + (\hat{v}_y - \bar{v}_y)^T\Gamma^{-1}(\dot{\hat{v}}_y + \Gamma y_e) + \tilde{u}_1\dot{\tilde{u}}_1 + (\hat{\eta}-\eta)^T\gamma^{-1}\dot{\hat{\eta}} \tag{5.40}$$

Substituting (5.31)(5.35)(5.36) into (5.40), we have the following equation

$$\begin{aligned}
&\dot{V}_2 \le -k_x x_e^2 - k_y y_e^2 - (\rho_1 - |\varepsilon_1|)|y_e| + y_e v_r\tilde{u}_1 + (\hat{v}_y - \bar{v}_y)^T\Gamma^{-1}(\dot{\hat{v}}_y + \Gamma y_e)\\
&+\tilde{u}_1\Big(\cos\theta_e\big(c(s)v_r - \frac{v_x}{l}\tan\delta + \frac{\bar{v}_y + \varepsilon_1}{l} - \frac{v_x}{l}(\eta + \varepsilon_2)\big) + \frac{1}{v_r}(\varpi\dot{y}_e - \dot{\hat{v}}_y)\Big)\\
&+(\hat{\eta}-\eta)^T\gamma^{-1}\dot{\hat{\eta}} + \zeta_1
\end{aligned} \tag{5.41}$$

where ζ_1 is a trivial variation due to the replacement of $sign()$ by tanh() in (5.35). In (5.41) $\dot{y}_e$ is substituted by the kinematic model with sliding (5.11b), the following equation can be obtained

$$\begin{aligned}
&\dot{V}_2 \le -k_x x_e^2 - k_y y_e^2 - (\rho_1 - |\varepsilon_1|)|y_e| + (\hat{v}_y - \bar{v}_y)^T\Gamma^{-1}(\dot{\hat{v}}_y + \Gamma y_e)\\
&+\tilde{u}_1\Big(y_e v_r + \cos\theta_e c(s)v_r - (\cos\theta_e\frac{v_x}{l} + \frac{\varpi x_e v_x}{v_r l})u_2 + \frac{1}{l}(\cos\theta_e + \frac{\varpi x_e}{v_r})(\bar{v}_y + \varepsilon_1) - \frac{\varpi\varepsilon_1}{v_r} + \frac{\varpi(v_r\sin\theta_e - \hat{v}_y) - \dot{\hat{v}}_y}{v_r}\Big)\\
&+(\hat{\eta}-\eta)^T\gamma^{-1}(\dot{\hat{\eta}} + \gamma\tilde{u}_1\beta) - \tilde{u}_1\beta\hat{\eta} - \tilde{u}_1\beta\varepsilon_2 - (\bar{v}_y - \hat{v}_y)\frac{\tilde{u}_1\varpi}{v_r} + \zeta_1
\end{aligned} \tag{5.42}$$

where β is defined by (5.47). By algebraic transformation the derivative of V_2 becomes

$$\begin{aligned}
&\dot{V}_2 \le -k_x x_e^2 - k_y y_e^2 - (\rho_1 - |\varepsilon_1|)|y_e| + (\hat{v}_y - \bar{v}_y)^T\Gamma^{-1}(\dot{\hat{v}}_y + \Gamma y_e)\\
&+\tilde{u}_1\Big(y_e v_r + \cos\theta_e c(s)v_r - (\cos\theta_e\frac{v_x}{l} + \frac{\varpi x_e v_x}{v_r l})u_2 + \tau(\hat{v}_y + \varepsilon_1) - \frac{\varpi\varepsilon_1}{v_r} + \alpha\Big) + \tilde{u}_1\tau(\bar{v}_y - \hat{v}_y)\\
&+(\hat{\eta}-\eta)^T\gamma^{-1}(\dot{\hat{\eta}} + \gamma\tilde{u}_1\beta) - \tilde{u}_1\beta\hat{\eta} - \tilde{u}_1\beta\varepsilon_2 - (\bar{v}_y - \hat{v}_y)\frac{\tilde{u}_1\varpi}{v_r} + \zeta_1
\end{aligned} \tag{5.43}$$

where α and τ are defined by (5.45) and (5.46). Finally the derivative of V_2 is simplified into

$$\begin{aligned}
&\dot{V}_2 \le -k_x x_e^2 - k_y y_e^2 - (\rho_1 - |\varepsilon_1|)|y_e| + \tilde{u}_1(\lambda - \beta u_2 + \alpha - \frac{\varpi\varepsilon_1}{v_r} - \beta\hat{\eta} + \tau\varepsilon_1 - \beta\varepsilon_2)\\
&+(\hat{v}_y - \bar{v}_y)^T\Gamma^{-1}(\dot{\hat{v}}_y + \Gamma y_e - \Gamma\tilde{u}_1\tau + \Gamma\frac{\varpi}{v_r}\tilde{u}_1)\\
&+(\hat{\eta}-\eta)^T\gamma^{-1}(\dot{\hat{\eta}} + \gamma\tilde{u}_1\beta) + \zeta_1
\end{aligned} \tag{5.44}$$

where

$$\alpha = \frac{\varpi(v_r\sin\theta_e - \hat{v}_y) - \dot{\hat{v}}_y}{v_r} \tag{5.45}$$

$$\tau = \frac{1}{l}(\cos\theta_e + \frac{\varpi x_e}{v_r}) \tag{5.46}$$

$$\beta = v_x\tau \tag{5.47}$$

$$\lambda = y_e v_r + \cos\theta_e c(s)v_r + \tau\hat{v}_y \tag{5.48}$$

In (5.44) let

$$\begin{aligned}
&\dot{\hat{\eta}} = -\gamma\tilde{u}_1\beta\\
&\dot{\hat{v}}_y = -\Gamma y_e + \Gamma\tilde{u}_1\tau - \Gamma\frac{\varpi}{v_r}\tilde{u}_1
\end{aligned} \tag{5.49}$$

and choose u_2 as

$$u_2 = \frac{1}{\beta}\Big(k_u\tilde{u}_1 + \lambda + \alpha - \beta\hat{\eta} + \rho_1\big(\frac{\cos\theta_e}{l} + \frac{\varpi}{v_r}\Big|\frac{x_e - l}{l}\Big|\big)\tanh(\frac{\tilde{u}_1}{\sigma_2}) + |\beta|\rho_2\tanh(\frac{\tilde{u}_1}{\sigma_3})\Big) \tag{5.50}$$

where $sign()$ has been substituted by $tanh()$ and $\sigma_i > 0$, then we get

$$\dot{V}_2 \leq -k_x x_e^2 - k_y y_e^2 - k_u\tilde{u}_1^2 - (\rho_1 - |\varepsilon_1|)|y_e| - (\rho_2 - |\varepsilon_2|)|\beta||\tilde{u}_1| - (\rho_1 - |\varepsilon_1|)(\frac{\cos\theta_e}{l} + \frac{\varpi}{v_r}\Big|\frac{x_e - l}{l}\Big|)|\tilde{u}_1| + \zeta \tag{5.51}$$

where $\zeta = \zeta_1 + \zeta_2$, ζ_2 is another trivial variation due to the substitution of $sign()$ by $tanh()$ in (5.50). (5.51) implies that the closed-loop system is uniformly bounded.

5.2.4 Stability Analysis

From (5.51) it is known that the longitudinal deviation x_e, lateral deviation y_e and $\tilde{u}_1$ are all bounded. Indeed all of them converge into a neighborhood of zero. The range of the neighborhood is determined by ζ which is linked to σ_i. The smaller σ_i is, the smaller the range of the neighborhood is, yielding higher accuracy.

When y_e and $\tilde{u}_1$ vary around zero, from (5.34) and (5.35) one gets that the orientation error θ_e converges into a neighborhood of

$$\theta_e = \arcsin\big(\frac{\hat{v}_y}{v_r}\big) \tag{5.52}$$

5.3 Simplified adaptive controller with projection mapping

The robust adaptive controller (5.50) with VSC can guarantee high tracking accuracy from academic point of view. But in actual applications due to limited bandwidth of agriculture vehicles and lag of hydraulic-drive steering systems, performances of the robust adaptive controller (5.50) may be deteriorated by significant "Chattering".

To be of more benefit to actual applications, the robust adaptive controller is simplified by setting ρ_i to zero, then we get $\varpi = k_y$ and the controller (5.50) is reduced into an ordinary adaptive controller without VSC components.

$$u_2 = \frac{1}{\beta}\Big(k_u\tilde{u}_1 + \lambda + \alpha - \beta\hat{\eta}\Big) \tag{5.53}$$

By using the similar Lyapunov's direct method, it is proven that the adaptive controller (5.53) leads to the following result

$$\dot{V}_2 = -k_x x_e^2 - k_y y_e^2 - k_u\tilde{u}_1^2 + \varepsilon_1(\frac{\tilde{u}_1\cos\theta_e}{l} - \frac{\tilde{u}_1 k_y}{v_r} - y_e) - \tilde{u}_1\cos\theta_e\frac{v_x}{l}\varepsilon_2 \tag{5.54}$$

In (5.54) the effect of ε_1 is introduced through its appearance in (5.29)(5.36), the effect of ε_2 is introduced by its appearance in (5.36). (5.54) implies the closed-loop system is uniformly bounded. But comparing with (5.51) in which only ζ is a negligible disturbance, (5.54) is subjected to all the unmodeled sliding effects.

To make the adaptive controller (5.53) more robust to the unmodelled sliding effects, projection mapping is used for the parameter adaptation procedure. The projection mapping $Proj_\xi(\bullet)$ is defined by [29, 30]

$$Proj_\xi(\bullet) = \begin{cases} 0 & if \;\; \hat{\xi} = \xi_{\max} \;\; and \;\; \bullet > 0 \\ 0 & if \;\; \hat{\xi} = \xi_{\min} \;\; and \;\; \bullet < 0 \\ \bullet & otherwise \end{cases} \tag{5.55}$$

By using the projection mapping $Proj_\xi(\bullet)$, the robust adaptive laws become

$$\dot{\hat{v}}_y = Proj_{\bar{v}_y}\big(-\Gamma y_e + \Gamma\tilde{u}_1\tau - \Gamma\frac{\varpi}{v_r}\tilde{u}_1\big) \tag{5.56}$$

$$\dot{\hat{\eta}} = Proj_\eta\big(-\gamma\tilde{u}_1\beta\big) \tag{5.57}$$

The prior information on the bounds of the sliding effects $\bar{v}_y, \eta$ can be obtained off-line after performing large number of absolute coordinates measurements under different typical working conditions.

5.4 Simulation Results

First a classical "U" path with a perfect circular arc (path #1) is applied as the reference trajectory to test the proposed controllers. In the simulations, the gains used in (5.31) and (5.50) are set as $k_x = 0.6$, $k_y = 0.15$, $k_u = 1.14$. The gains of the adaptive laws (5.49) as set as $\Gamma = 0.2$, $\gamma = 0.05$. In actual implementations these gains should be tuned gradually to make an optimal compromise between transient characteristic and limited bandwidth of the steering system. The reference velocity is set as $v_r = 8.4km/h$ which is the normal velocity of agriculture vehicles in agriculture applications.

In the first simulation the constant sliding is introduced with $v_y = -0.1$, $\delta_b = -0.048$. The control law (5.25) without considering sliding is applied also with the same controller gains. The simulation results of the longitudinal, lateral and orientation errors are shown by figure 5.2-5.4. Since the vehicle velocity is initialized to zero, obvious longitudinal errors are noticed at the beginning of the simulations. The initial orientation errors are also nonzero. Those initial errors quite fit with the real working conditions. From the simulations it is clear that all the controllers can make the longitudinal-lateral errors approach to zero before sliding occurs. But when sliding appears, because the control law (5.25) does not take sliding effects into account, the longitudinal-lateral deviations (dashed line) become significant. While the robust adaptive controller (5.50) can compensate sliding effects through estimating them on line and counteract modeling inaccuracy by VSC, so the longitudinal-lateral deviations can converge to zero with a good transient response (solid line). Finally the adaptive controller (5.53) is simulated also. (5.53) can compensate time-invariant sliding, the effects of the time-varying sliding are moderated by projection mapping, hence its longitudinal-lateral deviations (dotted line) converge to zero with small offsets (due to linearization approximation in (5.11c)). The remarkable overshoots at the beginning and end of the curve are caused by "jump change" of the sliding effects and low level delay. The bounded orientation errors are shown by figure 5.4. As analyzed by section 5.2.4 the proposed controllers cannot make the orientation errors converge to zero, indeed they are bounded around (5.52). It is normal when sliding occurs known as "crab sliding". The evolution of the sliding parameters $\hat{v}_y$ (solid line), $\hat{\eta}$ (dashed line) is displayed by figure 5.5. At the beginning and end of the circle, $\hat{v}_y$ varies greatly which explains the overshoots of the lateral deviation, but as the vehicle follows the circle, $\hat{v}_y$, $\hat{\eta}$ evolve smoothly close to the real values.

To simulate the actual working conditions, a set of real measurement data is used in the simulation to reconstruct the actual sliding effects v_y and δ_b. The longitudinal-lateral deviations are shown by 5.6, 5.7. The (robust) adaptive controllers yield small lateral deviations with zero mean value, while the lateral deviation of the controller (5.25) is significant and has obvious bias. The longitudinal errors of the (robust) adaptive controller are also less than it of (5.25). It is because when the lateral sliding and steering bias are compensated by (robust) adaptive controllers, the negative influences of y_e and θ_e (due to sliding) on the longitudinal tracking accuracy is moderated.

In order to fully present the proposed controllers, another realistic reference trajectory #2 which is sampled in an actual agriculture application is tracked (see figure 5.8). The longitudinal and lateral deviations are displayed by figure 5.9, 5.10. The experimental data indicates that although the trajectory #2 is more complex than trajectory #1, the proposed controllers can still track it with high accuracy in presence of sliding. Furthermore the robust adaptive controller with VSC yields better transient performances at the expense of non-smooth movements (solid line) especially when low level delay is considered. While the adaptive controller (5.53) with projection mapping yields a movement with less oscillation (dotted line), but its bias is larger than VSC's. So in case when sliding is dominant, the robust adaptive controller with VSC is favorable. But for the vehicles whose bandwidth is limited, the adaptive controller with projection mapping is preferred.

5.5 Conclusion

The problem of trajectory tracking control of autonomous agricultural vehicles in the presence of sliding is investigated in this chapter. A kinematic model which integrates the sliding effects as additive unknown parameters is constructed. From this model, a robust adaptive controller is designed based on backstepping methods which can stabilize the longitudinal-lateral derivations into a neighborhood of zero and guarantees the orientation error converge into a neighborhood near the origin. In addition a reduced adaptive controller with projection mapping is proposed for the purpose of smooth vehicle movements. Experimental comparative results show the effectiveness of the proposed control laws. The advantages of this scheme are that

- When no sliding occurs, the proposed controller can guarantee longitudinal-lateral deviations and orientation errors converge to zero.
- Integrating parameter adaptation with backstepping schemes yields a practical trajectory tracking controller for agriculture vehicles. Also it is applicable for platoon control.
- Backstepping procedures can be extended easily to high-order nonholonomic systems, for example trailer control.

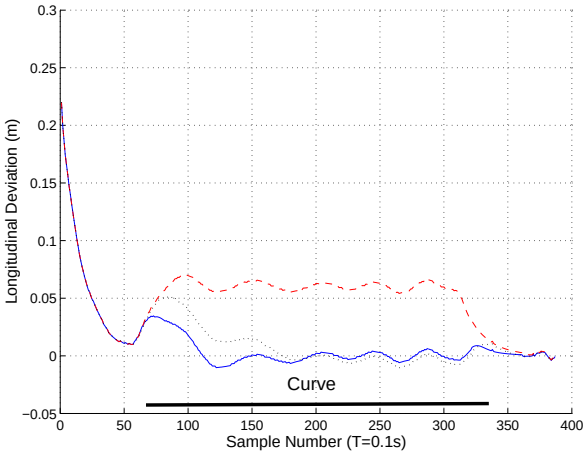

Figure 5.2: Longitudinal deviation of path #1

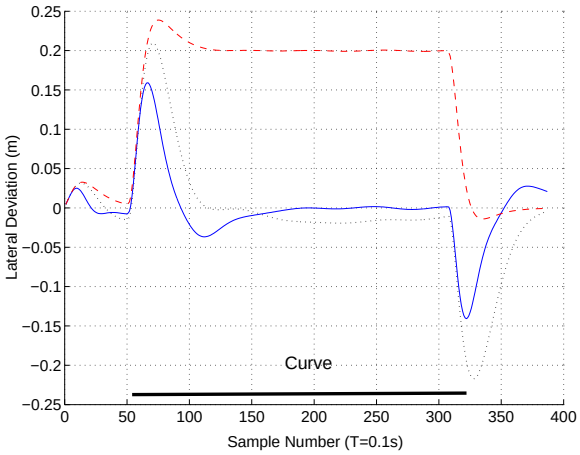

Figure 5.3: Lateral deviation of path #1

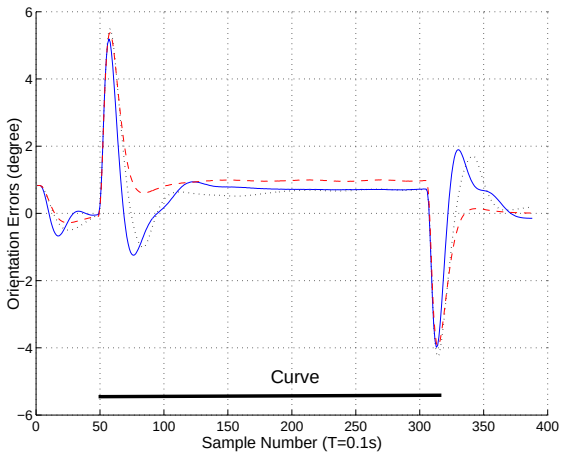

Figure 5.4: Orientation errors of path #1

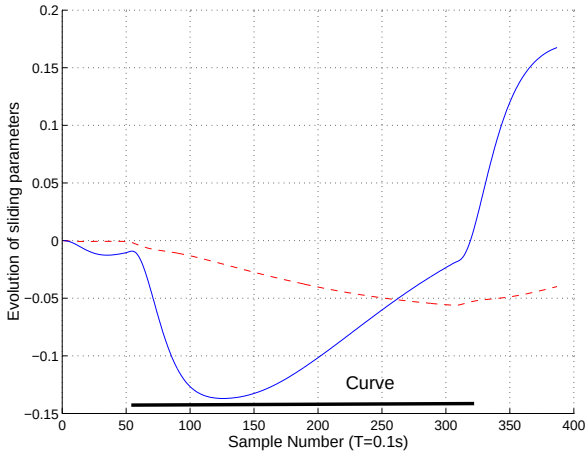

Figure 5.5: Evolution of sliding parameters

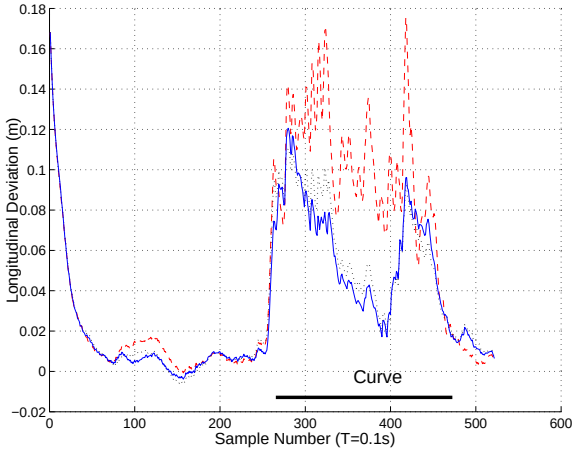

Figure 5.6: Longitudinal deviation of path #1 with real measurements

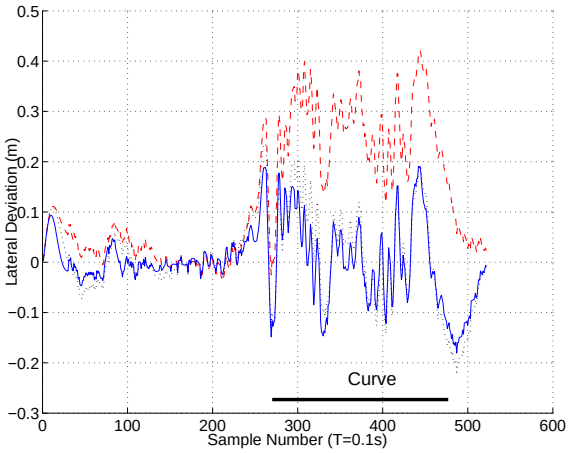

Figure 5.7: Lateral deviation of path #1 with real measurements

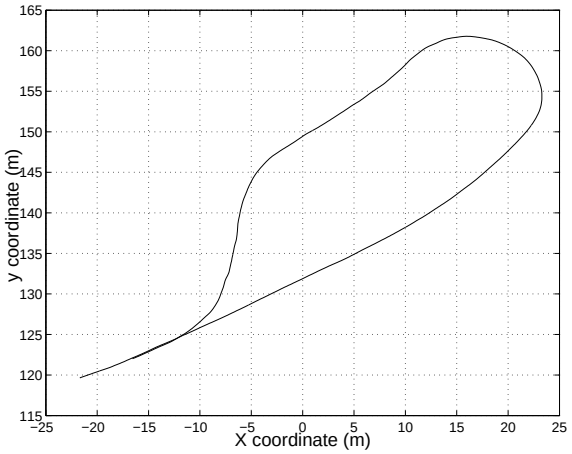

Figure 5.8: Path #2 to be followed

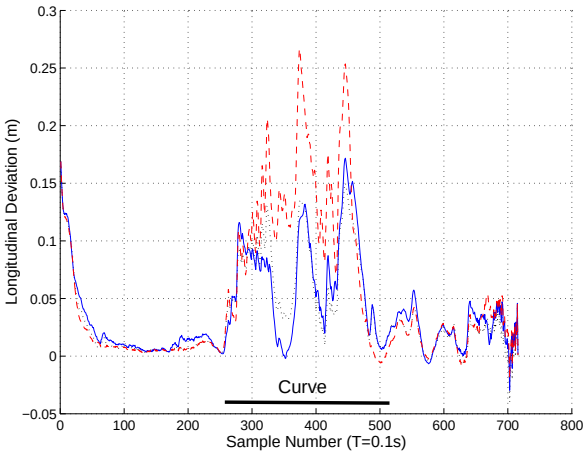

Figure 5.9: Longitudinal deviation of path #2 with real measurements

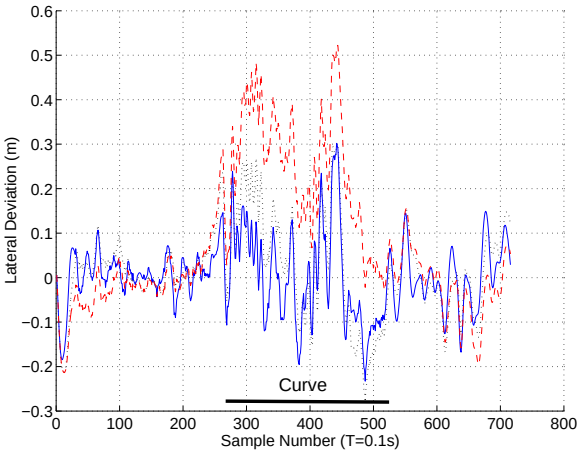

Figure 5.10: Lateral deviation of path #2 with real measurements

Chapter 6

SUMMARY AND FUTURE WORKS

6.1 Summary

The aim of this work is to design some advanced controllers for autonomous vehicles to guarantee them enough mobility including high lateral and longitudinal tracking accuracy when they move on several typical grounds. In order to face the facts that in real worlds pure rolling constraints are seldom strictly satisfied, this work expanded the previous work of [11] which is under the assumption of pure rolling. Several anti-sliding controllers have been developed. The numerical simulations have validated their effectiveness.

To take sliding effects into account, a kinematic and a dynamic models with sliding are constructed. The kinematic model is finally transformed into a specific form in which sliding appears as additive uncertainties to the ideal kinematic model. In the dynamic model uncertain sliding effects are indicated by corning stiffness coefficients. Although throughout this work all the controllers are designed based on the kinematic model, the structure of the resulting dynamic model is still beneficial to robust controller designing.

To facilitate GPS-based applications, this work has proven that all the state variables of the vehicle models can be measured or reconstructed with GPS. The detailed reconstruction schemes are rather easy and quite straightforward which is realistic for real applications.

Since the kinematic model with sliding have been obtained, it is intrinsic to regard sliding effects as external disturbances to the ideal kinematic model. Therefore robust control theories are utilized to design a controller which makes the vehicles robust to the sliding. On the other hand chained system properties are attractive for nonholonomic system control. They can transform a nonholonomic system into a linear system which allows us to use linear system theories to design a controller. So sliding mode control was combined with chained system theories to design a robust controller. It has been theoretically proven that the closed-loop system is globally uniformly bounded.

Robust controllers can remedy sliding effects in some degrees, but since all the sliding effects are counteracted only by adjusting the gains of the sliding mode controllers, the negative "Chattering" effects become significant especially for vehicles with time delay. Sometimes a smooth vehicle motion is more preferred than a high tracking accuracy. To share the undertaking of the sliding mode controller, a robust adaptive controller is designed. Backstepping has been proven effective in designing adaptive controllers for nonholonomic systems, so combination of backstepping schemes with variable structure control leads to a robust adaptive controller. In this controller the time-invariant sliding component is rejected by adaptive adaptation, while the variable structure controller is responsible for correcting the time-varying sliding component. Although its structure is more complex than the sliding mode controller's, the robust adaptive controller allows us to use low gain control which can yield a smooth vehicle motion. With Lyapunov's direct method, it is proven that the proposed robust adaptive controller make the lateral deviation stable in neighborhood of zero, the orientation error is stabilized into a neighborhood near the origin in presence of sliding.

Above two path following controllers can guarantee high lateral and orientation accuracy, but longitudinal control is very required for high-way vehicle safety and platoon control. Longitudinal-lateral control is the final target of this project, it is also the highlight of this work. First instead of building kinematic model with respect to the path frame, in longitudinal-lateral control the kinematic model is constructed in the vehicle body frame. Then a robust adaptive controller is designed similarly by combining backstepping schemes with variable structure control. Benefitting from the utilization of backstepping methods, the developing procedure

is quite easy and straightforward for understanding despite the complicated model of 2-3 nonholonomic systems with uncertainties. The resulting controller allows the lateral-longitudinal deviations to converge into a neighborhood of zero and the orientation error to be stabilized into a neighborhood near the origin in presence of sliding.

6.2 Future works

The prospective works include extending the backstepping methods to high-order nonholonomic system control. High-precision control for the general case of N trailers is still open. It may be one of the promising subjects for the application of backstepping. Furthermore platoon control also may be benefited from these works. The longitudinal-lateral controller can be applied directly to platoon control, what we need to do is just computing the "virtual reference vehicle" for each following vehicle based on the required safety distances and path curvature.

Utilize other techniques such as filter theories, signal processing, observer theories to identify system parameters in real time. It is very important for actual applications in which prior knowledge is very limited and iterative training is not allowed. In such cases real-time online system parameter identification has great sense, since it can improve adaptive control by offering accurate model parameters.

Refine kinematic models to concern about real vehicle systems, for example mechanical limitations, backlash at the steering wheels, actuator saturation and dead-zone, noise and biases of the sensors. All of them have important influence on the control accuracy. In this work we ignored them in the kinematic model which deteriorated the control accuracy in actual applications. There are two solutions to this problem. One is to refine the kinematic model to take into account all the important factors. Another is to improve the control robustness with respect to theses kinds of uncertainties. The latter seems to be more easily, but it is still an open and challenging subject of research.

Throughout this study we have dealt with a kinematic model in which velocity and steering angle were assumed to be the control inputs. But for heavy vehicles and high-speed vehicles, dynamics is no longer negligible. The inherent relationships between vehicles and grounds can be explained clearly only by dynamic models. So for high-precision automatic guidance, the dynamic model of vehicles, tires and actuators are very necessary. In future works kinematic models should be extended to integrate dynamic models with generalized forces as inputs. We have obtained a dynamic model whose structure is convenient for application of robust control. But the exact dynamic model describing internal reaction between different kinds of grounds and vehicles is still not available.

Bibliography

[1] Stombaugh, T. S. , *Automatic Guidance of Agricultural Vehicles at Higher Speeds*, Ph.D. dissertation. Dept. of Agriculture Engineering, University of Illinois at Urbana-Champaign, 1997.

[2] Samson, C "Control of chained systems, Application to path following and time-varying point stabilization of mobile robot", *IEEE Trans,on Automatic Control*, 39(12):2411-2425,1995.

[3] Billingsley, J. and Schoenfisch, M. " Vision-Guidance of Agricultural Vehicles", *Autonomous Robots*, 2, pp. 65-76, 1995.

[4] G. Elkaim, M. OConner, T. Bell and B. Parkinson, "System Identification and Robust Control of Farm Vehicles Using CDGPS", IONGPS-97, Kansas City, MO, USA, Vol 2:1415-1424, 1997.

[5] Reid, J. F., "Precision Guidance of Agricultural Vehicles", SME Meeting, Sapporo, Japan. UILU-ENG-7031,1998.

[6] Wit, J., "Vector Pursuit Path Tracking for Autonomous Ground Vehicles," Ph.D. dissertation, University of Florida, 2000.

[7] J. Ackermann, "Robust control prevents car skidding", *IEEE Control Systems Magazine*, pages 23-31, June 1997

[8] I. Motte, H. Campion, "Control of sliding mobile robots : a slow manifold approach", MNTS 2000

[9] O Conner, M., Bell, T., Elkaim, G. and Parkingson, B., "Automatic Steering of Farm Vehicles Using GPS", *in Proceedings of the 3rd International Conference on Precision Agriculture*, June 1996 .

[10] G. Elkaim, M. OConner, T. Bell and B. Parkinson, "System Identification and Robust Control of Farm Vehicles Using CDGPS", IONGPS-97, Kansas City, MO, USA, Vol 2:1415-1424, 1997.

[11] Thuilot B, Cariou C, Martinet P, and Berducat M, "Automatic guidance of a farm tractor relying on a single CP-DGPS", *Autonomous robots* , 13(1): 87-104,2002

[12] L. Cordesses, P. Martinet, B. Thuilot and M. Berducat, "GPS-based Control of a Land Vehicle",*16th International Symposium on Automation & Robotics in Construction*, IAARC99, Madrid, Spain, September 22-24, 1999

[13] W. Leroquais, B. D'Andrea-Novel, " Vibrational control of wheeled mobile robots not satisfying ideal velocity constraints: the unicycle case ", *European Control Conference*, July 1-4, Brussels,1997

[14] Y. L. Zhang, J. H. Chung, S. A. Velinsky, " Variable structure control of a differentially steered wheeled mobile robot", *Journal of intelligent and Robotic Systems*, 36:301-314,2003

[15] M. L. Corradini and G. Orlando, "Experimental testing of a discrete-time sliding mode controller for trajectory tracking of a wheeled mobile robot in the presence of skidding effects", *Journal of robotic systems*, 19(4), 177-188, 2002

[16] B. D'Andrea-Novel, G. Campion and G. Bastin. "Control of wheeled mobile robots not satisfying ideal constraints: a singular perturbation approach", *International Journal of Robust Nonlinear Control*, 5:243-267,1995.

[17] Lenain R. Thuilot B. Cariou C, Martinet P. "Adaptive control for car like vehicles guidance relying on RTK GPS: rejection of sliding effects in agricultural applications", *In Proc. of the intern. Conf. On Robotics and Automation*, Taipei, Sept, 2003.

[18] N. Matsumoto and M.Tomizuka, "Vehicle lateral velocity and yaw rate control with two independent control inputs", *Trans. of the ASME -J. of dynamic systems, measurement, and control*, 114:606-613, Dec, 1992

[19] M.G. Mehrabi, R. M.H. Cheng, and A. Hemami, "Control of a wheeled mobile robot with double steering ", *In IEEE Conf. On Intelligent Robots & Systems*, 806-810, Osaka, Nov, 1991.

[20] M. L. Corradini and G. Orlando, "Robust tracking control of mobile robots in the presence of uncertainties in the dynamics model", *Journal of robotic systems*, 18(6), 317-323, 2001

[21] Z. P. Jiang and H. Nijmeijer, "A recursive technique for tracking control of nonholonomic systems in chained form",*IEEE Transactions on Automatic Control*, vol. 44, no. 2, 265-279, 1999.

[22] Kanellakopoulos, and P. Kokotovic, *Nonlinear and Adaptive Control Design*, John Wiley and Sons, ISBN: 0-471-12732-9, 1995.

[23] Y. P. Zhang, B. Fidan, P. A. Ioannou, " Backstepping control of linear time-varying systems with known and unknown parameters",*IEEE Trans. Auto Contr.*, vol.48, pp. 1908-1925,2003

[24] T.Floquet, J-P.Barbot, W.Perruquetti, "One-chained form and sliding mode stabilization for nonholonomic perturbed systems", Proceeding of the American Control Conference, Chicago,Illinois,:3264-3268,June 2000

[25] J.Lu, S.Sekhavat, M. Xie,and C.Laugier, "Sliding mode control for nonholonomic mobile robot", *In Proc. of the Int. Conf. on Control, Automation, Robotics and Vision*, Singapore, December 2000.

[26] N. Matsumoto and M. Tomizuka, " Vehicle lateral velocity and yaw rate control with two independent control inputs", *Trans. of the ASME -J. of dynamic systems, measurement, and control*, 114:606-613, Dec, 1992

[27] M. G. Mehrabi, R. M. H. Cheng, and A. Hemami, " Control of a wheeled mobile robot with double steering ", *IEEE Conf. On Intelligent Robots & Systems*, 806-810, Osaka, Nov, 1991.

[28] Koshkouei, A. J. Zinober, A. S. I. " Adaptive Backstepping Control of Nonlinear Systems with Unmatched Uncertainty", *Proceedings of the 39th IEEE Conference on Decision and Control* , Sydney, pp. 4765-4700, 2000

[29] B. Yao and M. Tomizuka, "Smooth robust adaptive sliding mode control of robot manipulators with guaranteed transient performance, *Trans. of ASME, Journal of Dynamic Systems, Measurement and Control*, vol. 118, no. 4, pp. 764–775, 1996.

[30] S. Sastry, M. Bodson, *Adaptive Control: Stability, Convergence, and Robustness*, Prentice-Hall, ISBN 0-13-004326-5, 1989

[31] Lenain R. Thuilot B. Cariou C, Martinet P. "Model Predictive Control of vehicle in presence of sliding Application to farm vehicles path tracking", Submitted to ICRA05.

[32] Ryu, C., Gerdes, J.C., " Vehicle Sideslip and Roll Parameter Estimation Using GPS", *AVEC, Hiroshima, Japan*, 2002.